이학박사학위논문

ULK1 당화에 의한 자가포식작용 조절에 대한 연구

Studies on the Regulation of Autophagy Initiation by ULK1 O-GlcNAcylation

2018 년 8 월

서울대학교 대학원

생명과학부

표 기 은

Studies on the Regulation of Autophagy Initiation by ULK1 O-GlcNAcylation

by

Ki Eun Pyo

Advisor

Professor Sung Hee Baek, Ph.D.

A Thesis for the Degree of Doctor of Philosophy

June, 2018

School of Biological Sciences

Seoul National University

ABSTRACT

Ki Eun Pyo
School of Biological Sciences
Graduate Course
Seoul National University

Unc-51-Like-Kinase 1 (ULK1) is a target of both mechanistic target of rapamycin (mTOR) and AMP-activated protein kinase (AMPK) whose role is to facilitate initiation of autophagy in response to starvation. Upon glucose starvation, dissociation of mTOR from ULK1 as well as phosphorylation by AMPK leads to activation of ULK1 activity. Here, I provide evidence that ULK1 is O-GlcNAcylated on threonine 754 site by O-linked N-acetylglucosamine transferase (OGT) upon glucose starvation. Surprisingly, ULK1 O-GlcNAcylation requires dephosphorylation of adjacent mTOR-dependent phosphorylation on Serine 757 site by protein phosphatase 1 (PP1) and phosphorylation by AMPK. O-GlcNAcylation of ULK1 is crucial for ATG14L phosphorylation and activation of lipid kinase VPS34, leading to production of phosphatidylinositol-(3)-phosphate (PI(3)P) required for phagophore formation and subsequent initiation of autophagy. Together, my findings provide new insights into the crosstalk between dephosphorylation and O-GlcNAcylation

during autophagy process and specify a molecular framework for potential therapeutic intervention in autophagy-related diseases.

Keywords

Autophagy, Unc-51-like-Kinase 1 (ULK1), O-linked N-acetylglucosamine transferase (OGT), Mechanistic target of rapamycin (mTOR), AMP-activated protein kinase (AMPK), Protein Phosphatase 1 (PP1)

Student Number: 2010-23128

CONTENTS

LIST OF FIGURES AND TABLES (in the order of appearance)

CHAPTER I

Introduction

I-1 Autophagy

1.1 The autophagy pathway

Autophagy is an intracellular degradation system which delivers unnecessary cytoplasmic constituents or pathogens to the lysosome for recycling. One of the most fundamental and evolutionarily conserved functions of autophagy is its role in response to nutrient starvation. In budding yeast, autophagy is suppressed to undetectable levels under growing conditions. However, it is rapidly induced during nitrogen starvation. This same type of response is also observed in higher organisms (Mizushima, 2007).

Besides starvation adaptation, there are a wide variety of physiological processes affected by autophagy, such as intracellular protein and organelle clearance, apoptosis, elimination of microorganisms, and tumor suppression (Mizushima, 2005). In the case of neurons, constitutive degradation of cytosolic contents by autophagy is indispensable, even in the absence of disease-associated mutant protein expression (Mizushima et al., 2008). In the case of apoptosis, autophagy deficiency results in the increased generation of apoptotic cells during development (Qu et al., 2007). Moreover, autophagy is implicated in elimination of microorganisms. Intracellular bacteria, viruses, and protozoans are removed from host cells by autophagy, and antigens are processed for MHC class II antigen presentation (Levine and Deretic, 2007). Autophagy also

suppresses tumor by removing damaged organelles and possibly growth factors, and by reducing chromosome instability (Mathew et al., 2007).

Autophagy is mediated by a unique organelle called the autophagosome. Unlike ubiquitin-proteasome pathway which specifically recognizes only ubiquitinated proteins for degradation, autophagy is generally considered as a nonselective degradation system because the autophagosome engulfs a portion of cytoplasm (Mizushima et al., 2008). Although the capacity for large-scale degradation is critical in autophagic function, too much degradation may be lethal for the cell. On the other hand, basal levels of autophagy are necessary for maintaining normal cellular homeostasis. Therefore, either too little or too much autophagy can be deleterious for the cell.

1.2 Autophagy initiation

In yeast, autophagosomes originate from a single preautophagosomal structure. Although an equivalent structure has not been reported in mammalian cells, a special subdomain in the endoplasmic reticulum termed the “omegasome” has been suggested as a putative origin of autophagosomes. This structure is enriched in PI(3)P, a product of the phosphatidylinositol 3-kinase (PI3K) class III complex. A hierarchical analysis of the mammalian ATG proteins confirmed the recruitment of ULK1 proximal to these omegasomes (Hara et al., 2008). The translocation of ULK1, in a complex with ATG13 and FIP200, to the omegasomes is the initial step of autophagosome biogenesis.

Overall, autophagy consists of several sequential steps: initiation, phagophore formation, transportation of autophagosomes to lysosomes, cargo degradation, and utilization of degradation products.

First, cytoplasmic constituents including old proteins, lipids, and organelles are sequestered by a unique membrane called the phagophore or isolation membrane, which is a very flat organelle. Complete sequestration of the cytoplasmic constituents by the elongating phagophore leads to formation of the autophagosome, which is a double-membraned organelle (Mizushima, 2007). At this stage, no degradation of cytoplasmic constituents occurs. After closure, autophagosomes fuse with lysosomes to expose their content to the hydrolases originating from the interior of the lysosomes and cytoplasmic constituents are degraded (Fig. I-1).

The compositions of the outer and inner autophagosomal membranes are quite different. For example, LC3, a mammalian homolog of Atg8, has been identified on the autophagosomal inner membrane (Mizushima, 2007). LC3 has been proposed to function as a receptor for a selective substrate, p62. p62 has both LC3-binding and ubiquitin-binding domains, allowing it to mediate the recognition of ubiquitinated protein aggregates by LC3 within the autophagosome (Pankiv et al., 2007). Moreover, p62 markedly accumulates in autophagy-deficient cells, indicating that it is selectively recognized and degraded by autophagy. On the outer autophagosomal membrane, the *N*-ethylmaleimide-sensitive factor attachment protein receptor (SNARE) Syntaxin 17 (STX17) promotes autophagosome–lysosome fusion by interacting with SNAP-29 and the lysosomal SNARE VAMP8 (Fig. I-2) (Itakura et al., 2012).

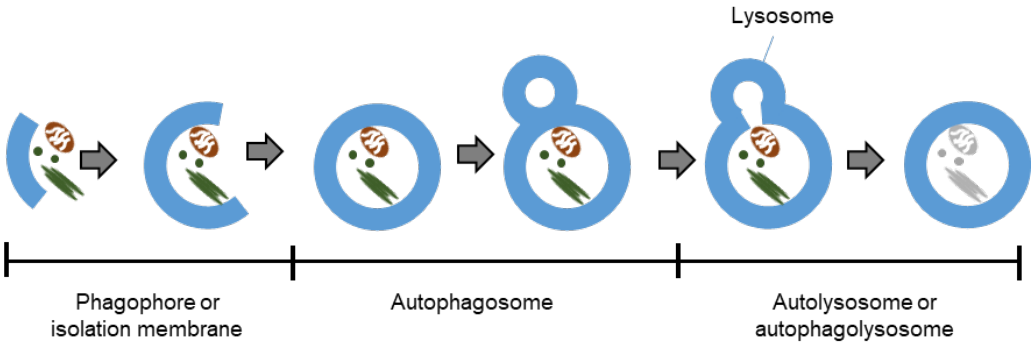

Figure I-1. The process of macroautophagy in mammalian cells.
A portion of cytoplasm, including organelles, is enclosed by a phagophore or isolation membrane to form an autophagosome. The outer membrane of the autophagosome subsequently fuses with the endosome and then the lysosome, and the internal material is degraded (Mizushima, 2007).

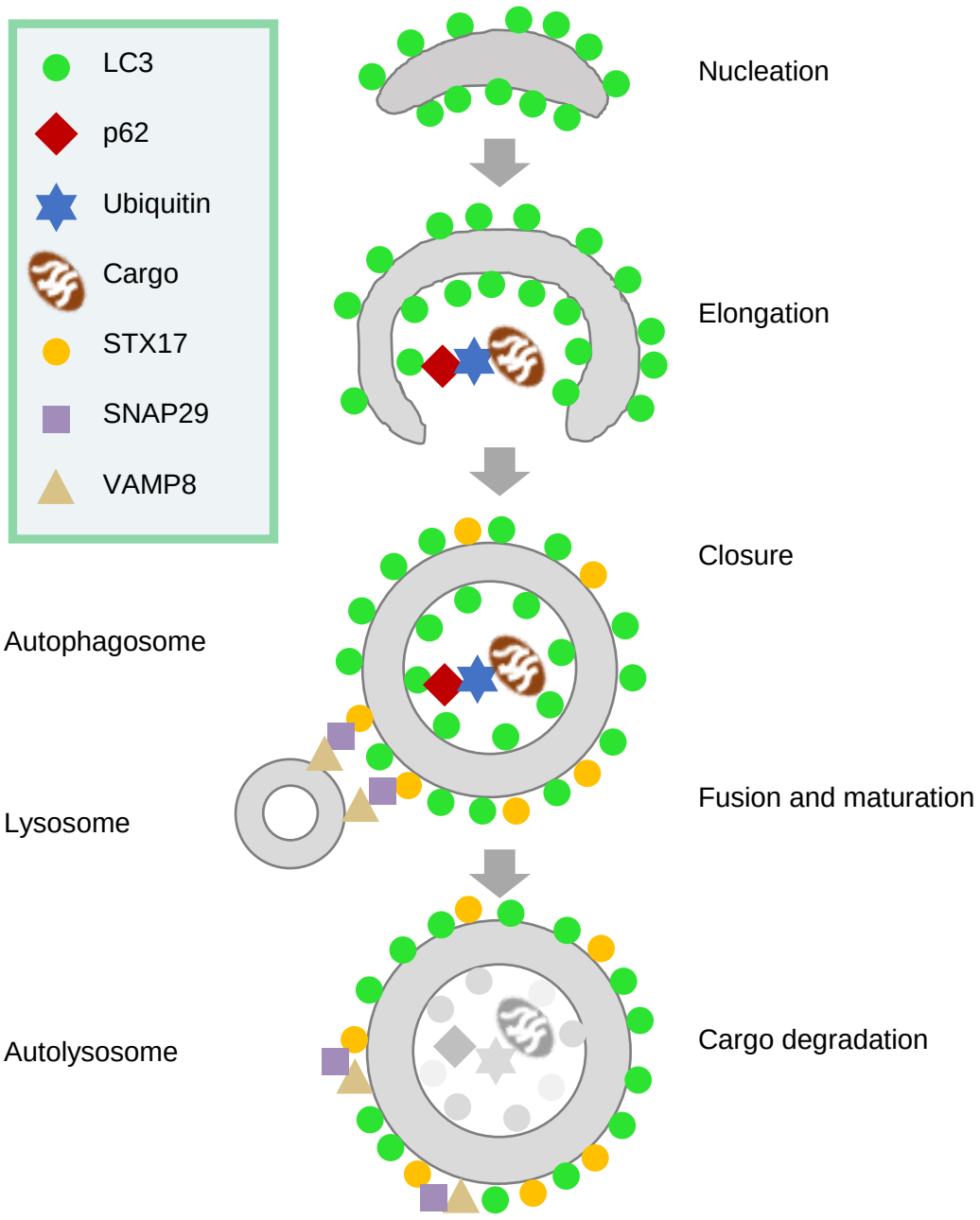
LC3
p62
Ubiquitin
Cargo
STX17
SNAP29
VAMP8
Nucleation
Elongation
Closure
Autophagosome
Fusion and maturation
Lysosome
Cargo degradation
Autolysosome

Figure I-2. Formation and maturation of autophagosome
Autophagy regulators such as BECLIN1, ATG14, and VPS34 function in membrane nucleation to form the double-membraned phagophore. Additional autophagy-related proteins such as ATG7 and ATG5 mediate the elongation step, in which the phagophore begins to expand until it closes around the cytoplasmic constitnuents targeted for degradation. The closed autophagosome fuses with lysosomes via the soluble N-ethylmaleimide-sensitive factor attachment protein receptor (SNARE) complex consisting of syntaxin 17 (STX17), SNAP29, and VAMP8. The engulfed contents as well as the inner membrane in the newly formed autolysosome are degraded, in a process termed autophagic flux.

I-2. Unc-51-Like-Kinase 1 (ULK1)

1.1 ULK1 is a serine/threonine kinase

Phosphorylation is a type of post-translational modification found in a variety of cellular proteins that has been implicated in cellular growth, mitosis, and response to DNA damage. Although proteins are covalently modified in many other ways, including methylation, ubiquitination, acetylation, glycosylation, hydroxylation, tyrosine sulfation and sumoylation, none of these mechanisms is nearly as widespread and readily subject to regulation by various stimuli as is phosphorylation.

Phosphate groups are highly negatively charged. This feature of phosphorylation leads to alteration of the protein's charge, which can also lead to alteration of the conformation and ultimately functional activity. Kinases phosphorylate substrate proteins, and phosphatases dephosphorylate substrate proteins. A change in the state of protein phosphorylation occurs through increased or decreased activity of either kinases or phosphatases.

Kinases are classified into three groups: serine/threonine kinases, tyrosine kinases, and dual-function kinases. Serine/threonine kinases phosphorylate substrate proteins on serine or threonine residues. Tyrosine kinases phosphorylate substrate proteins on tyrosine residues. Dual-function kinases phosphorylate substrate proteins on both serine/threonine and tyrosine residues. Statistical analysis revealed that over 95% of protein phosphorylation occurs on serine residues, 3 to 4% on threonine residues and

less than 1% on tyrosine residues (Nestler et al, 1999). In particular, serine/threonine kinase enzymes phosphorylate the OH group of serine or threonine, which have similar side chains. At least 125 of the 500 human protein kinases are serine/threonine kinases (Capra et al., 2006).

ULK1 has a serine-threonine kinase domain at its N terminus and domain of unknown function at its C-terminus. The kinase domain is conserved among different species such as yeast and mammals (Yan et al., 1998). ULK1 is heavily phosphorylated, and requires autophosphorylation for stability.

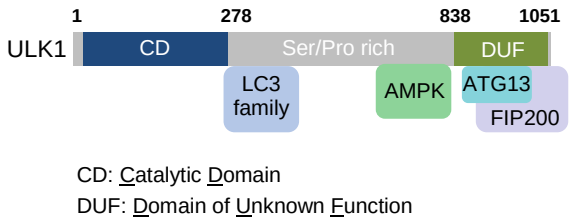

Figure I-3 Domains within ULK1 and known binding regions
ULK1 contains a catalytic domain (CD), a domain of unknown function (DUF) that is conserved with the yeast and *C. elegans* counterparts, and a serine/proline-rich region in between which is the site for many post-translational modification events. ATG13 and FIP200 interact with ULK1 through its DUF. The mapped interaction sites with members of the LC3 family and AMPK are indicated.

1.2 Functions of ULK1 during autophagy

Pioneering studies in budding yeast identified 36 genes required for autophagy, most of which are conserved in mammals. One of the most upstream genes identified in yeast was ATG1. By far, ATG1 is the only autophagy gene to encode a serine/threonine kinase. In mammals, there are two Atg1 homologs, ULK1 and ULK2. Several groups have reported that ULK1 complex is activated in response to nutrient deprivation and serves as a critical initiator of starvation-induced autophagy (Egan et al., 2011; Kim et al., 2011; Russell, 2013; Shang and Wang, 2011).

ULK1 forms a multiprotein complex by interacting with ATG13, FIP200 and ATG101. The ULK1 complex engages in the formation of omegasomes, the phosphatidylinositol-3-phosphate (PI(3)P)-enriched membrane platform from which phagophores form. Although the localization of most of the other ATG proteins does not depend on the catalytic activity of ULK1, it is nonetheless essential for the formation of autophagosomes (Alers et al., 2012). Also, the recruitment of the PI3K class III complex (VPS34 complex) to the phagophore depends on ULK1 and its kinase activity.

ULK1 is phosphorylated by mechanistic target of rapamycin serine/threonine kinase complex 1 (mTORC1) and AMP-activated protein kinase (AMPK). Interestingly, AMPK-mediated phosphorylations are required for full activation of ULK1, whereas mTORC1-mediated phosphorylations prevent AMPK-mediated phosphorylations and activation of ULK1 (Park et al., 2016).

Several studies have confirmed the positive regulation of ULK1 activity through AMPK-dependent phosphorylation. S555 in ULK1 is one of the major AMPK-

dependent phosphorylation sites. In addition, several other sites of AMPK-dependent phosphorylation have been identified, such as S317, S467, T574, S637, and S777. Among them S317 and S777 are known to regulate the kinase activity of ULK1. S467, S555, T574 are sites responsible for regulating mitochondrial homeostasis during starvation. S637 is the site where both mTORC1 and AMPK phosphorylate.

Being direct targets of both mTORC1 and AMPK, ULK1 regulation is unlikely mutually exclusive. It might induce conformational changes to increase kinase activity, change the interaction with other regulatory components, such as 14-3-3 proteins, AMPK, and mTORC1, and/or affect the subcellular localization.

Residue	Kinase	Functional Effect
T180	ULK1	Stimulates ULK1 kinase activity
S317	AMPK	Stimulates ULK1 kinase activity
S467	AMPK	Required for mitochondrial homeostasis during starvation
S555	AMPK	Required for mitochondrial homeostasis during starvation
T574	AMPK	Required for mitochondrial homeostasis during starvation
S637	mTORC1 AMPK	Promotes ULK1–AMPK interaction, Required for mitochondrial homeostasis during starvation
S757	mTORC1	Inhibits ULK1 kinase activity
S777	AMPK	Stimulates ULK1 kinase activity

Table I-1. Phosphorylated residues on ULK1
As many as 30 phosphorylation events have been reported for ULK1. For simplicity, only events that have been experimentally verified are listed in the table.

I-3 Mechanistic target of rapamycin (mTOR)

1.1 Regulation of cellular metabolism and growth by mTOR

The mTOR signaling pathway is one of the master regulators of cell growth that integrates multiple inputs such as growth factors, nutrients, hypoxia, endoplasmic reticulum stress, and energy depletion (Benjamin and Hall, 2014). It has been considered as a critical integral mechanism linking metabolic disorders, cancer, and aging.

mTOR is the catalytic subunit of two structurally distinct complexes: mTORC1 and mTORC2. Both complexes localize to different subcellular compartments, thus affecting their activation and function. mTORC1 functions as a nutrient, energy, and redox sensor and controls protein synthesis. It consists of mTOR catalytic subunit and four associated proteins, including regulatory associated protein of mTOR (RAPTOR), mammalian lethal with sec13 protein 8 (mLST8), proline-rich Akt substrate of 40 kDa (PRAS40), and Deptor (Julien et al., 2010). In contrast, mTORC2 functions as an important regulator of the actin cytoskeleton (Hay and Sonenberg, 2004), consisting of mTOR, rapamycin-insensitive companion of mTOR (RICTOR), mammalian stress-activated mitogen-activated protein kinase-interacting protein 1 (mSin1), mLST8, proline-rich region 5 (PRR5), and Deptor (Julien et al., 2010). In both complexes, mTOR functions mainly as a serine/threonine kinase, although in mTORC2 it also functions as a tyrosine kinase. In addition, RAPTOR and RICTOR function as scaffold proteins for

assembling mTORC1 and mTORC2, binding substrates, and their respective regulators (Zoncu et al., 2011).

In particular, mTORC1 enhances protein synthesis through its downstream targets S6K1 and eIF4E-binding protein 1 (4E-BP1). Once phosphorylated by mTORC1, 4E-BP1 dissociates from eIF4E, thereby relieving its suppression of mRNA translation. Simultaneously, mTORC1-dependent S6K1 phosphorylation promotes mRNA translation. Also, mTORC1 induces lipogenesis in the liver through activation of transcription factors SREBP1 and PPARγ, inhibits autophagy through phosphorylation of the ULK1–Atg13–FIP200 complex, and promotes mitochondrial biogenesis through activation of PGC1α/YY1 (Zoncu et al., 2011).

Interesting observations have been reported regarding mTORC1 deactivation. For example, chemical inhibitors of glycolysis and mitochondrial function suppress mTORC1 activity (Kim et al., 2002). This suggests that energy depletion stops mTORC1 signaling pathway, and prevents consuming too much energy for growth while the cell is on the brink of survival. More importantly, two independent studies have suggested that mTORC1 deactivation is an acute, active process and not merely a dampening of mTORC1 signaling due to dissipation of its upstream stimuli (Demetriades et al., 2014; Menon et al., 2014). The abrupt deactivation when no longer needed demonstrates that mTORC1 activity is tightly controlled and suggests a corresponding level of control for mTORC1 downstream effectors such as the S6K1, 4EBP, and ULK1 proteins. Phosphatases responsible for dephosphorylation of these mTORC1 target proteins, and

their acute stimulation under mTORC1-inactivating conditions have been hypothesized, yet little evidence has been reported.

1.2 Regulation of ULK1 by mTOR

Growth factors activate the PI3K/AKT pathway through receptor tyrosine kinases. Upon growth factor binding, AKT is recruited to the plasma membrane, where it is activated through phosphorylation by PDK1. Activated AKT phosphorylates tuberous sclerosis complex 2 (TSC2), which prevents formation of the inhibitory TSC1/TSC2 heterodimer. Since TSC2 serves as a GTPase-activating protein and inactivates the small GTPase Rheb, its inhibition subsequently allows Rheb to activate mTORC1 (Alers et al., 2012). mTORC1 is recruited to lysosomes in a Rag-dependent manner upon amino acid stimulation, where it is finally activated by Rheb GTPases.

So far, yeast genetic screenings for autophagy defective mutants have led to the identification 36 essential autophagy-related genes (ATG). Most upstream is a protein complex that comprises the serine/threonine kinase ATG1 (yeast homolog of ULK1), as well as two accessory proteins ATG13 and ATG17. ATG1 complex is directly regulated by TORC1 (yeast homolog of mTORC1) in a nutrient-dependent manner. In mouse, mTORC1 phosphorylates ULK1 on S757 thereby keeping ULK1 serine/threonine kinase inactive and preventing initiation of autophagy.

While the yeast TORC1 was reported to disrupt the complex formation of the yeast form of ULK1, mammalian mTORC1 does not have a similar effect on the ULK1–ATG13–FIP200 complex (Jung et al., 2009). However, the interaction between ULK1

and AMPK is disrupted by mTORC1 (Kim et al., 2011). Based on the fact that AMPK activates ULK1 during glucose starvation, it is possible that phosphorylation of ULK1 by mTORC1 is one of the factors influencing the interaction between ULK1 and AMPK.

I-4 AMP-activated protein kinase (AMPK)

1.1 Functions of AMPK during autophagy

AMPK is a serine/threonine kinase and is regarded as a major nutrient sensor. AMPK is activated either when it is directly phosphorylated by Liver Kinase B1 (LKB1), or when intracellular ATP level decreases whereas AMP and ADP level increase. At low levels of ATP, AMP and ADP directly bind to γ regulatory subunit of AMPK, leading to activation of AMPK followed by a variety of catabolic processes such as glucose uptake and metabolism. Once activated, it simultaneously inhibits several anabolic pathways, such as lipid, protein, and carbohydrate biosynthesis (Hardie, 2007).

In accordance with catabolic functions, AMPK is also linked to the regulation of autophagy. In addition to AMPK's activation by low cellular energy levels via LKB1 and high AMP and ADP concentrations, it has been suggested that various non-starvation-related autophagy-inducing stimuli primarily act through the activation of AMPK even under normal energy levels. Although the expression of a dominant-negative form of AMPK completely inhibited autophagic proteolysis in HT-29 and HeLa cells under harsh starvation conditions such as Hanks balanced salt solution (HBSS),

transfection with a constitutively active (CA) form of AMPK did not affect the rate of autophagy (Meley et al., 2006). Thus, it is still not clear whether AMPK activation alone is sufficient to induce autophagy in mammalian cells, or whether the basal activity of AMPK, although essential for autophagy induction, must be accompanied by additional cell stress such as nutrient withdrawal.

I-5 O-linked N-acetylglucosamine transferase (OGT)

1.1 OGT is a glycosyltransferase

Throughout evolution organisms have developed ways to sense nutrients in their surroundings through a robust network of signaling pathways, and one of them is O-GlcNAcylation. O-GlcNAc glycosylation of proteins on serine and threonine residues depends on the flux of glucose through the hexosamine biosynthetic pathway (HBP). A fraction (2 to 5%) of the glucose entering the cell is directed into this pathway for the biosynthesis of UDP-GlcNAc. OGT utilizes UDP-GlcNAc as a substrate to add GlcNAc on serine or threonine residues of the target protein, and its activity is highly dependent on the concentration of UDP-GlcNAc in the cell. These modifications can be reversed by O-GlcNAcase (OGA), which removes the O-GlcNAc moiety from O-GlcNAc-modified proteins (Kanwal et al., 2013). There are many targets identified so far, which are both nuclear and cytoplasmic targets.

The OGT enzyme is post-translationally modified, including O-GlcNAcylation and tyrosine phosphorylation. It has 11 protein-protein interaction domains known as tetratricopeptide (TPR) repeats and it specifically interacts with various other proteins. Disruption of OGT activity is lethal in mouse embryonic stem cells, suggesting that O-GlcNAcylation is essential for survival.

O-GlcNAc is a single N-acetylglucosamine attached to the hydroxyl group of serines or threonines in a number of intracellular proteins. However, evidence is accumulating for a regulatory interplay between phosphorylation and O-GlcNAc modifications. Although O-GlcNAc site consensus motif has not yet been identified, many attachment sites are identical to those used by serine/threonine kinases, and a neural network program has been developed to predict O-GlcNAc sites. Unlike phosphorylation, O-GlcNAc modification of tyrosine residues has yet to be observed.

1.2 Crosstalk between O-GlcNAcylation and phosphorylation

OGT exists in stable and active complexes with the serine/threonine phosphatases PP1β and PP1γ, enzymes that remove phosphate from proteins (Wells et al., 2004). The existence of this complex highlights the possible importance of understanding the dynamic relationship between *O*-GlcNAcylation and phosphorylation in modulating protein functions in various signaling cascades and regulations.

O-GlcNAc and O-phosphate site-mapping studies suggest that there are at least three different types of dynamic interplay between O-GlcNAc and O-phosphate. First,

there is competitive occupancy at the same site, as in the case of c-Myc, oestrogen receptor-β, and oncoprotein SV-40 large T-antigen (Cheng et al., 2000; Kamemura et al., 2002; Medina et al., 1998). Second, competitive and alternative occupancy occur at adjacent sites, such as that observed in the tumour suppressor p53 (Yang et al., 2006). Third, there is a complex interplay whereby some O-phosphate attachment sites on a given protein are the same as some O-GlcNAc sites, whereas others are adjacent to or distant from each other, such as on the C-terminal domain of RNA polymerase II and on cytokeratins (Chou et al., 1992; Comer and Hart, 2001).

What has been experimentally demonstrated so far by numerous groups suggests that the system is not binary (Hart et al., 2007). In other words, there is no 'on' or 'off' state for each molecule being controlled by both O-GlcNAcylation and phosphorylation. Rather, the combination of modifications creates enormous molecular diversity in contrast to when only one type of modification is available.

1.3 Stress-induced functions of OGT

One of the earliest responses to cellular stress is a rapid and global increase in O-GlcNAcylation on many proteins (Zachara and Hart, 2004). Stress-induced increases in O-GlcNAc are dynamic, returning to normal after 24–48 hours. Decreased OGT or global O-GlcNAc levels results in cells that are less stress tolerant, whereas increased OGT or gobal O-GlcNAc levels results in cells that are more viable after severe stress. Thus, short term increase in O-GlcNAcylation may be an important cell survival mechanism (Zachara and Hart, 2004). Some examples of stress-induced O-GlcNAc

modification change include T cell activation, insulin signaling, glucose metabolism, and cell cycle progression (Wells et al., 2001).

1.4 Physiological functions of OGT

Accumulating evidence suggests that there is a link between aberrant O-GlcNAc modification and type II diabetes (Wells et al., 2001). One of the hallmarks of type II diabetes is hyperglycemia, which is associated with an inability to trigger glucose uptake. Given that the activity of OGT is exquisitely responsive to intracellular UDP–GlcNAc, which is highly sensitive to glucose concentrations, increased levels of extracellular glucose and glucosamine lead to elevated intracellular O-GlcNAc modification of proteins in skeletal muscle and in pancreatic beta cells (Yki-Jarvinen et al., 1998).

In addition, numerous studies have linked O-GlcNAc cycling to the proteotoxicity associated with neurodegeneration, type II diabetes mellitus, and cardiovascular disease (Cole and Hart, 2001; Hart et al., 2007; Lehman et al., 2005). In the case of neurodegenerative diseases, several neuron-specifc phosophoproteins have been identified as targets of OGT, such as tau and β-amyloid precursor protein, both of which are implicated in Alzheimer's disease, as well as neurofilaments (Arnold et al., 1996; Dong et al., 1996; Griffith et al., 1995).

It is likely that alterations in O-GlcNAc cycling may also contribute to the pathology of other human diseases such as cancer. For example, overexpression of OGT or OGA causes mitotic exit defects in HeLa cells, and disrupts the normal timing of

cyclin protein expression and mitotic phosphorylation (Slawson et al., 2005). Since dysregulated cell cycle is one of the essential features of cancer cells, this observation suggests possible relevance of O-GlcNAcylation in cancer.

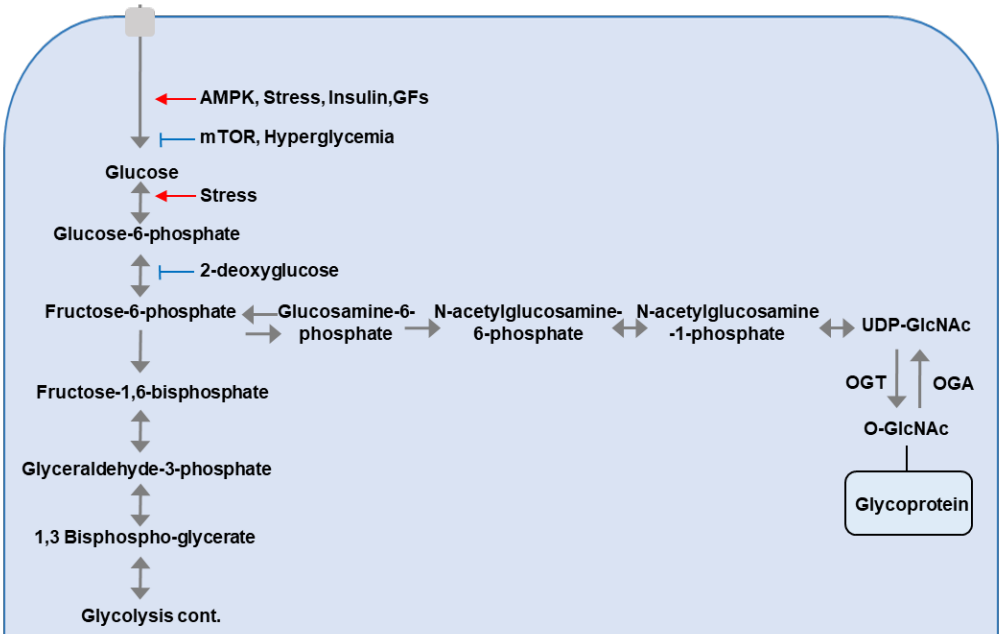

Figure I-4. The hexosamine biosynthetic pathway controls O-GlcNAc-modification of proteins.
O-GlcNAc glycosylation of proteins on serine and threonine residues depends on the flux of glucose through the hexosamine biosynthetic pathway (HBP). A fraction (2 to 5%) of the glucose entering the cell is directed into this pathway for the biosynthesis of UDP-GlcNAc.

CHAPTER II.

Increased ULK1 O-GlcNAcylation is positively correlated to autophagosome formation during glucose starvation

II-1. Summary

There have been speculations that OGT may work closely with phosphatases since O-GlcNAcylation and phosphorylation share the same target residues serine and threonine, and therefore are most likely antagonistic to each other, such as in the cases of CRTC2, p53, and CK2 proteins (Cheng and Hart, 2001; Chou et al., 1995; Dentin et al., 2008; Du et al., 2001; Tarrant et al., 2012; Yang et al., 2006).

Here, I provide evidence that ULK1 is O-GlcNAcylated by OGT on T754 site during glucose starvation, and that this modification is crucial for autophagosome formation. Through mutant studies and electron transfer dissociation (ETD) mass spectrometric analysis, I verified that ULK1 is O-GlcNAcylated on T754 site. Moreover, I observed the increased binding between ULK1 and OGT upon glucose starvation, and the subsequent O-GlcNAcylation by OGT was in conjunction with the increased LC3 II levels.

In parallel with the preceding observation, the total numbers of both autophagosomes and autolysosomes were significantly reduced when T754N mutant was reconstituted in contrast to WT reconstitution, indicating that ULK1 O-GlcNAcylation positively regulates autophagosome formation during glucose starvation. In addition, I gathered evidence for consecutive dephosphorylation and O-GlcNAcylation, where O-GlcNAcylation occurs after ULK1 phosphorylation on S757 is significantly diminished.

II-2. Introduction

There are two major upstream regulators of ULK1: the mechanistic target of rapamycin complex 1 (mTORC1) and AMPK. mTORC1 is a protein complex consisting of mTOR serine/threonine kinase, Raptor, MLST8, PRAS40, and DEPTOR. It functions as an ATP- and amino acid-sensor to balance nutrient availability and cell growth and the activation of mTORC1 inhibits autophagy (Mizushima et al., 2010). Conversely, AMPK regulates cellular metabolism to maintain energy homeostasis and promotes autophagy. ULK1 is phosphorylated on S757 site by mTOR in nutrient rich conditions, inhibiting ULK1 activation via disrupting its binding to AMPK (Hosokawa et al., 2011; Mizushima et al., 2010). Upon glucose starvation, AMPK inhibits mTORC1 and phosphorylates ULK1 to activate it and consequently enable autophagy initiation. Thus, AMPK and mTORC1 regulate autophagy through coordinated phosphorylation of ULK1.

O-GlcNAcylation is the covalent attachment of N-acetylglucosamine (GlcNAc) sugars to serine or threonine residues of protein substrates. It is catalyzed by a single enzyme, termed OGT, which transfers N-acetylglucosamine from UDP-GlcNAc to protein substrates. On the other hand, a single enzyme known as O-GlcNAcase (OGA), rapidly removes the O-GlcNAcylation from protein substrates (Slawson and Hart, 2011; Vocadlo, 2012). These two opposing enzymes dynamically alter the posttranslational modification state and protein functions in response to various signals and cellular processes. OGT is enriched in the nucleus, yet it is also present in the cytosol (Zeidan

and Hart, 2010). Insights into the function of OGT has more extensively come from studies focusing on O-GlcNAcylation of nuclear proteins such as histone H2B, histone modifying enzymes such as EZH2 and HDAC1, and transcription factors such as OCT4 and SOX2 (Chen et al., 2013; Chu et al., 2014; Jang et al., 2012; Zhu et al., 2016).

There have been speculations that OGT may work closely with phosphatases since O-GlcNAcylation and phosphorylation share the same target residues serine and threonine, and therefore are most likely antagonistic to each other, such as in the cases of CRTC2, p53, and CK2 proteins (Cheng and Hart, 2001; Chou et al., 1995; Dentin et al., 2008; Du et al., 2001; Tarrant et al., 2012; Yang et al., 2006). In support of this idea, OGT and phosphatases such as PP1β and PP1γ have been co-purified, although common targets of OGT and such phosphatases have not been identified thus far (Wells et al., 2004). Also, it is notable that while kinases regulating ULK1 phosphorylation are well documented, the only phosphatase that has been reported is PP2A, which dephosphorylates ULK1 on S637 site (Wong et al., 2015).

II-3. Results

ULK1 is O-GlcNAcylated by OGT on threonine 754 site

Since ULK1 functions as an important gatekeeper for the initiation of autophagy, I decided to look for possible upstream regulators of ULK1. Unexpectedly, I found that ULK1 and OGT interact with each other. Co-immunoprecipitation assay using antibody against ULK1 revealed that ULK1 bound to OGT at endogenous expression level (Fig. II-1A). I generated *ULK1*$^{-/-}$ HEK293 cells using CRISPR/Cas9 and confirmed the specific interaction between ULK1 and OGT (Fig. II-1B). This led me to speculate that ULK1 may be a target of OGT. To verify whether O-GlcNAcylation occurs on ULK1, *in vitro* OGT assay was performed. Indeed, introduction of OGT induced O-GlcNAcylation of ULK1 (Fig. II-1C). Also, treatment of cells with the OGA inhibitor, Thiamet G, increased ULK1 O-GlcNAcylation, while the total protein level of ULK1 did not change (Fig. II-1D).

Next, I set out to identify the site of O-GlcNAcylation on ULK1. Several deletion mutants of ULK1 were tested for O-GlcNAcylation. Full length, Δ279-833 which has 279-833 amino acid (aa) region deleted, 1-600 aa, and 279-833 aa were expressed in HEK293 cells and immunoprecipitated for O-GlcNAc band detection. ULK1 was O-GlcNAcylated only in the 601-833 aa region (Figure II-1E). Immunoblot results confirmed that threonine 754 is the major site of O-GlcNAcylation (Fig. II-1F).

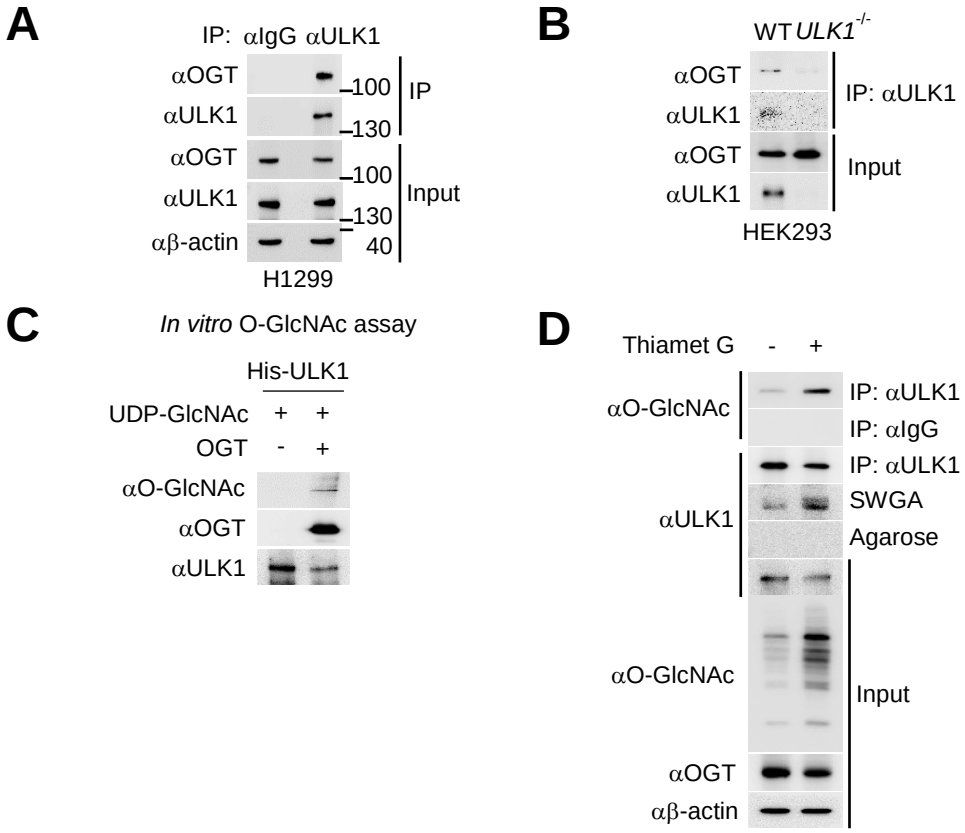
A
IP: αIgG αULK1
αOGT
αULK1
αOGT
αULK1
αβ-actin
100
130
100
130
40
IP
Input
H1299
B
WT ULK1-/-
αOGT
αULK1
αOGT
αULK1
IP: αULK1
Input
HEK293
C
In vitro O-GlcNAc assay
His-ULK1
UDP-GlcNAc + +
OGT - +
αO-GlcNAc
αOGT
αULK1
D
Thiamet G - +
αO-GlcNAc
αULK1
αO-GlcNAc
αOGT
αβ-actin
IP: αULK1
IP: αIgG
IP: αULK1
SWGA
Agarose
Input

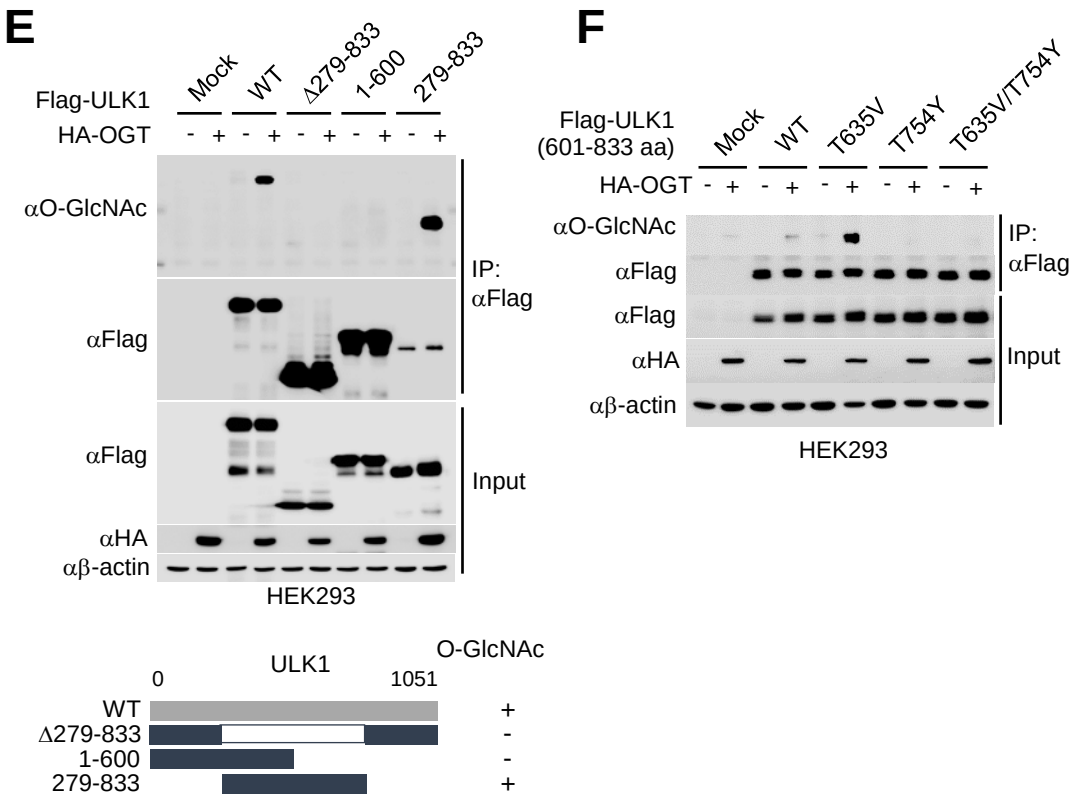

Figure II-1. ULK1 is O-GlcNAcylated by OGT

(**A**) Co-immunoprecipitation of endogenous ULK1 with OGT in H1299 cells. (**B**) Co-immunoprecipitation assay between ULK1 and OGT in WT or ULK1-/- HEK293 cells. (**C**) Detection of ULK1 O-GlcNAcylation after in vitro O-GlcNAcylation assay. (**D**) H1299 cells were treated with OGA inhibitor, Thiamet G (1 μM), followed by either pulldown of O-GlcNAcylated proteins using succinyl wheat germ agglutinin (SWGA) or immunoprecipitation to detect ULK1 O-GlcNAcylation. (**E**) ULK1 WT or deletion mutants including Δ279-833, 1-600, and 279-833 aa were tested for O-GlcNAcylation. (**F**) ULK1 WT or point mutants T635V, T754Y, and T635V/T754Y were pulled down with anti-Flag antibody and their O-GlcNAcylation band was detected.

ULK1 is O-GlcNAcylated by OGT

I went further to confirm the exact site of O-GlcNAcylation by electron transfer dissociation (ETD) mass spectrometric analysis and verified that ULK1 is O-GlcNAcylated on threonine 754 site which is well-conserved across species (Fig. II-2A and B). In addition, three different T754 mutants (T754A, T754N, and T754Y) of ULK1 were tested. First, I mutated threonine to alanine (A). Yet being close to mTOR-mediated serine 757 (S757) phosphorylation site, I also decided to mutate T754 to asparagine (N) or tyrosine (Y) since these amino acids are conserved mTOR target motif sequences in the corresponding position (Hsu et al., 2011). I reasoned that mTOR-mediated phosphorylation at S757 site should not be neglected because previous studies have shown that mTOR phosphorylates ULK1 in nutrient rich conditions, while upon starvation, ULK1 phosphorylation by mTOR is diminished, which releases ULK1 from inactive state (Kim et al., 2011). Therefore, several versions of conserved-motif-based T754 mutants were made in order to make sure mTOR-dependent phosphorylation occurs appropriately. In support of the ETD mass spectrometry data, co-immunoprecipitation and immunoblot analyses confirmed ULK1 O-GlcNAcylation on T754 since only WT but not T754Y, T754N, or T754A was O-GlcNAcylated (Fig. II-2C). Unexpectedly, I observed T754A mutant having diminished S757 phosphorylation dynamics, which would affect the precise mechanistic study on the interplay between O-GlcNAcylation by OGT and phosphorylation by mTOR (Fig. II-2D). Hereafter, I used T754N mutant to explore the function of ULK1 O-GlcNAcylation.

A

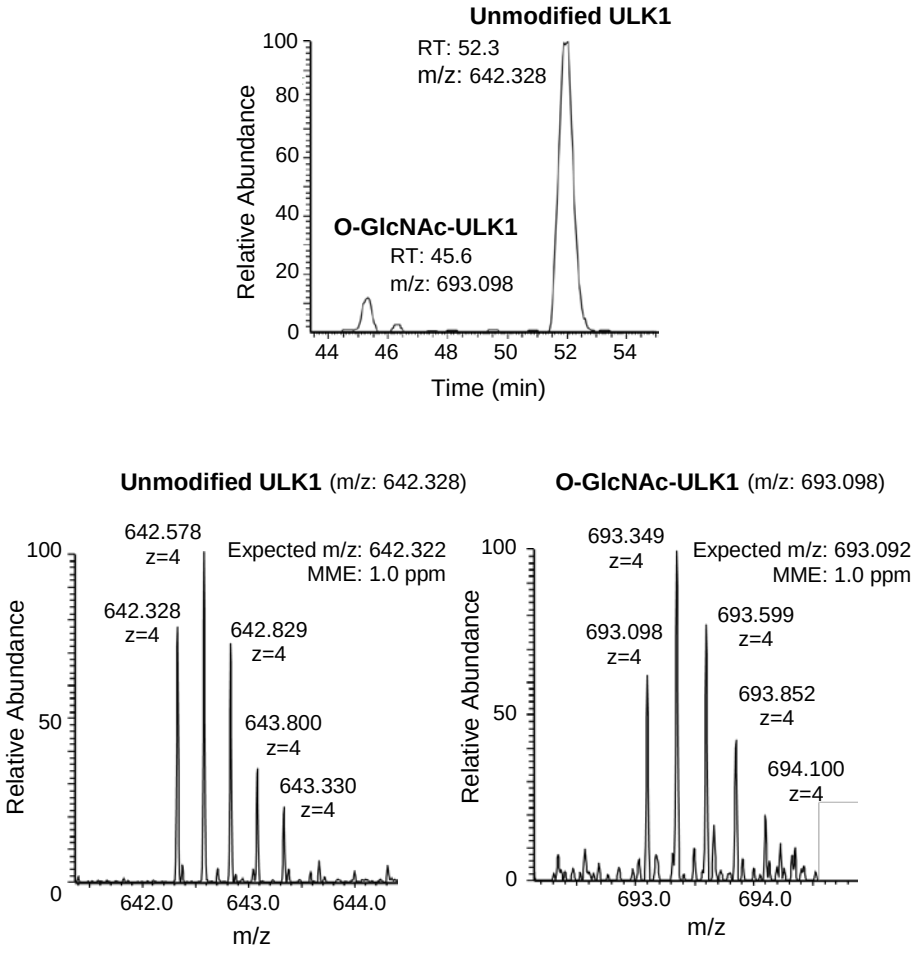
Unmodified ULK1
RT: 52.3
m/z: 642.328
O-GlcNAc-ULK1
RT: 45.6
m/z: 693.098
Relative Abundance
Time (min)
Unmodified ULK1 (m/z: 642.328)
642.578 z=4
Expected m/z: 642.322
MME: 1.0 ppm
642.328 z=4
642.829 z=4
643.800 z=4
643.330 z=4
m/z
O-GlcNAc-ULK1 (m/z: 693.098)
693.349 z=4
Expected m/z: 693.092
MME: 1.0 ppm
693.098 z=4
693.599 z=4
693.852 z=4
694.100 z=4

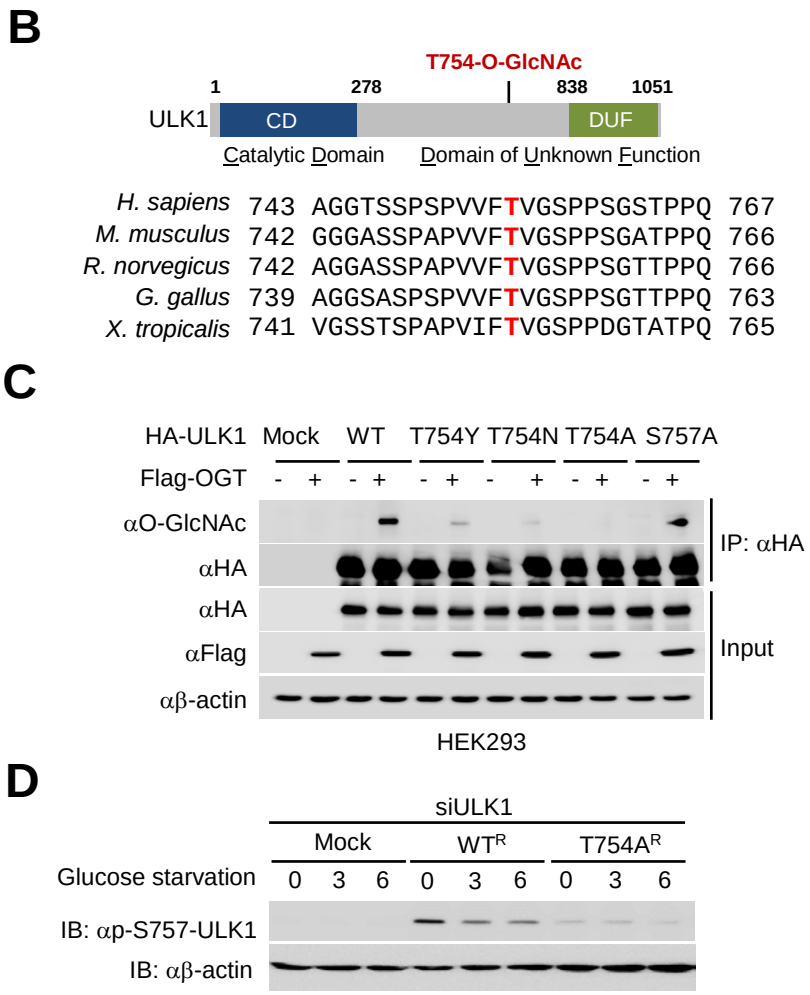

Figure II-2 ULK1 is O-GlcNAcylated by OGT on threonine 754 site
(**A**) ETD mass spectrometry analysis revealed the site of O-GlcNAcylation within ULK1 is threonine 754. (**B**) The site of ULK1 O-GlcNAcylation is conserved throughout species. (**C**) Threonine 754 mutated to tyrosine (Y), asparagine (N), or alanine (A), respectively. A residue other than T754, such as S757, was also mutated to alanine to validate the site of O-GlcNAcylation by co-immunoprecipitation. (**D**) T754A mutant had defects in S757 phosphorylation and was excluded for functional study

ULK1 O-GlcNAcylation occurs during glucose starvation

ULK1 activity largely depends on the availability of nutrients, and nutrient starvation conditions such as glucose starvation increase ULK1 activity (Kim et al., 2011; Shang and Wang, 2011). Therefore, I examined whether ULK1 and OGT interaction is affected by glucose starvation. Several different cell lines including H1299, HEK293, and SW620 similarly showed increased binding between ULK1 and OGT upon glucose starvation (Fig. II-3A). In parallel, ULK1 O-GlcNAcylation levels increased during glucose starvation, which was in conjunction with LC3 II conversion, a marker for autophagosomes and autolysosomes (Fig. II-3B), indicating that ULK1 O-GlcNAcylation has positive correlation with autophagy occurrence in these cell lines. Furthermore, I reasoned that if glucose levels and ULK1 O-GlcNAcylation levels have inverse correlation, reversing glucose levels in the media would reverse ULK1 O-GlcNAcylation levels. Indeed, glucose starvation followed by glucose repletion resulted in the reversal of the modification, with marked decrease of ULK1 O-GlcNAcylation levels after restoration of glucose in the media (Fig. II-3C). I also confirmed that ULK1 O-GlcNAcylation band disappeared when free N-acetyl D-glucosamine (NADG, mimics free UDP-GlcNAc) was added to the SWGA bead but no such band appeared in the *ULK1*$^{-/-}$ HEK293 cells, indicating that O-GlcNAcylation band is specific to ULK1 (Fig. II-3D).

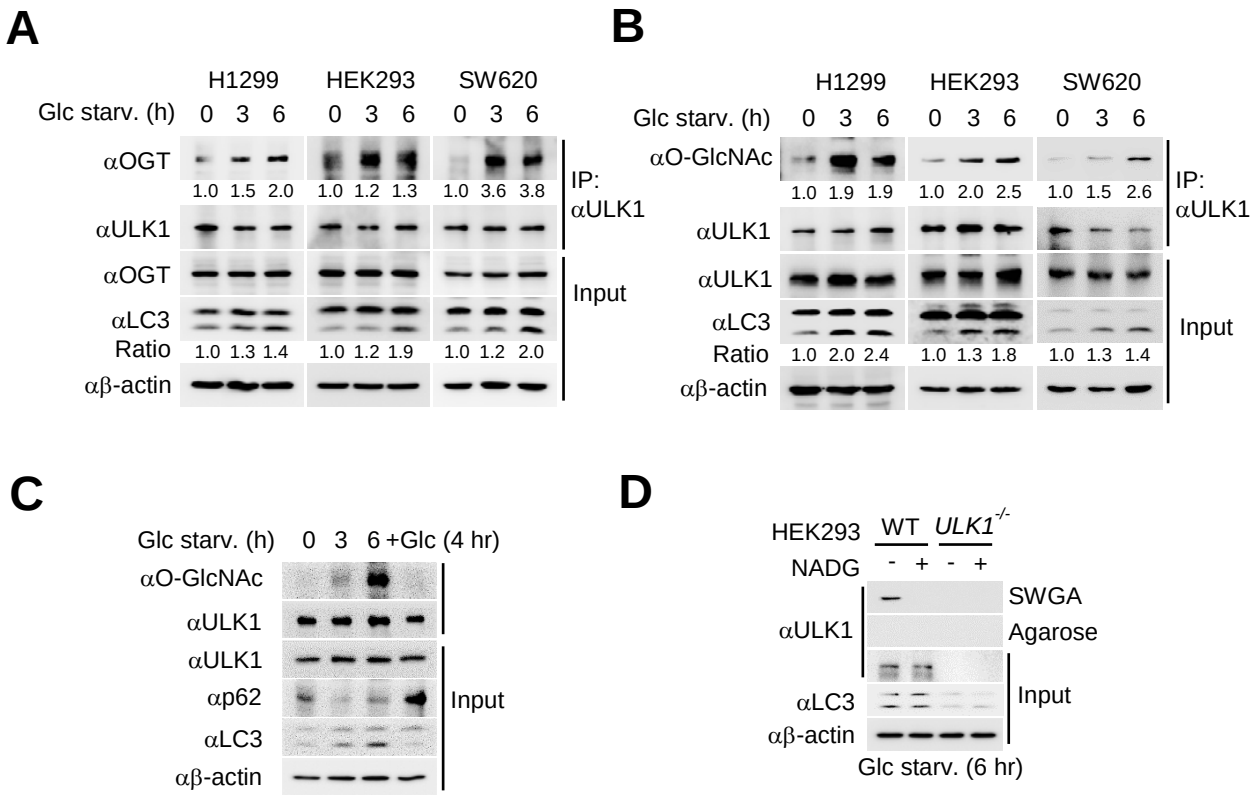

Figure II-3. ULK1 O-GlcNAcylation occurs during glucose starvation
(**A** and **B**) Glucose starvation for indicated times in H1299, HEK293, and SW620 cells. Samples were co-immunoprecipitated against anti-ULK1 antibody and either endogenous OGT or O-GlcNAcylation levels were detected. The LC3-II/β-actin ratio is indicated. (**C**) H1299 cells were glucose-starved and resupplied for 4 hours before harvest. (**D**) WT HEK293 cells were compared with *ULK1*$^{-/-}$ HEK293 cells to confirm ULK1-specific O-GlcNAcylation. SGWA beads were used to detect O-GlcNAcylation with or without N-acetyl D-glucosamine (NADG) which mimics free form of UDP-GlcNAc.

Increased ULK1 O-GlcNAcylation is positively correlated to autophagosome formation during glucose starvation

I further examined whether knockdown of OGT would result in the reduction of ULK1 O-GlcNAcylation levels and subsequently lead to inhibition of autophagy. First, I confirmed dramatically decreased ULK1 O-GlcNAcylation levels over the course of starvation when OGT was knocked down by siRNA (Fig. II-4A). Next, I used GFP-LC3 puncta as readout for autophagy occurrence, and found that the number of GFP-LC3 puncta decreased when OGT level was diminished, further indicating that OGT knockdown inhibits autophagosome formation (Fig. II-4B). To more precisely assess whether ULK1 O-GlcNAcylation modulates autophagosome formation, ULK1 was knocked down using siRNA and then siRNA-resistant ULK1 WT or T754N mutant was reconstituted. The mCherry-GFP-LC3 reporter was used to assess the overall number of LC3 puncta formation as well as autophagic flux. The GFP is attenuated in the acidic lysosomal environment, whereas the mCherry is not. Therefore, this reporter allows distinction between autophagosomes (GFP+/mCherry+ yellow puncta) and autolysosomes (GFP/mCherry+ red puncta). The total numbers of both autophagosomes and autolysosomes were significantly reduced when T754N mutant was reconstituted in contrast to WT reconstitution (Fig. II-4C), indicating that ULK1 O-GlcNAcylation positively regulates autophagosome formation. Bafilomycin A_1, which inhibits the fusion between autophagosomes and lysosomes, was used to assess autophagic flux. Treatment with bafilomycin A_1 resulted in significantly increased autophagosomes for both WT and T754N mutant. This increased number of nascent autophagosomes unable

to fuse with lysosomes indicates that the major function of ULK1 O-GlcNAcylation lies at the early steps of autophagy progression (Fig. II-4C).

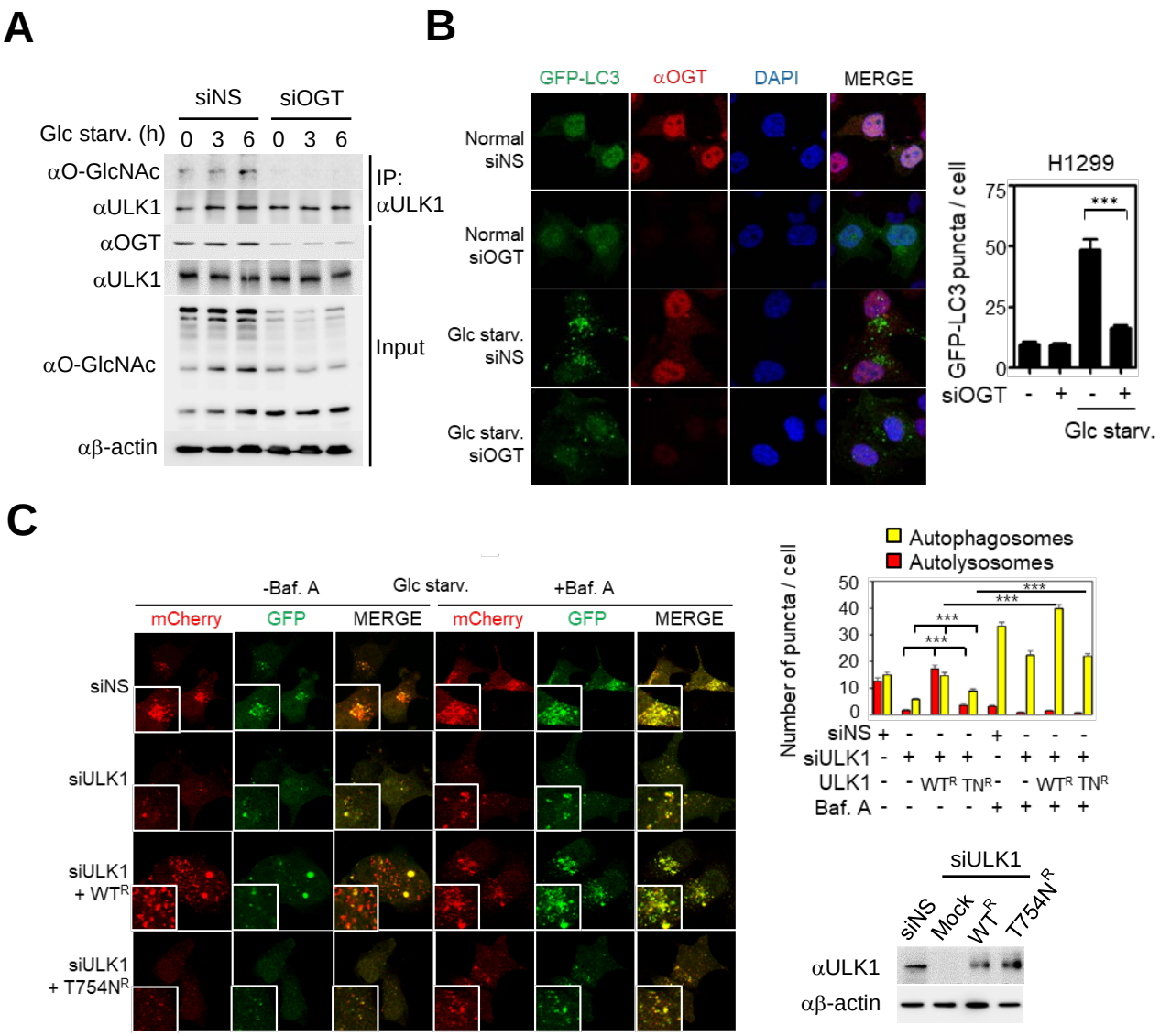
A
siNS
siOGT
Glc starv. (h)
0 3 6 0 3 6
αO-GlcNAc
αULK1
IP: αULK1
αOGT
αULK1
αO-GlcNAc
Input
αβ-actin
B
GFP-LC3
αOGT
DAPI
MERGE
Normal siNS
Normal siOGT
Glc starv. siNS
Glc starv. siOGT
H1299
GFP-LC3 puncta / cell
75
50
25
0
***
siOGT - + - +
Glc starv.
C
-Baf. A
Glc starv.
+Baf. A
mCherry
GFP
MERGE
mCherry
GFP
MERGE
siNS
siULK1
siULK1 + WTR
siULK1 + T754NR
Autophagosomes
Autolysosomes
Number of puncta / cell
50
40
30
20
10
0
***
***
***
***
siNS + - - - + - - -
siULK1 - + + + - + + +
ULK1 - - WTR TNR - - WTR TNR
Baf. A - - - - + + + +
siULK1
siNS
Mock
WTR
T754NR
αULK1
αβ-actin

Figure II-4. Increased ULK1 O-GlcNAcylation is positively correlated to autophagosome formation during glucose starvation

(**A**) Knockdown of nonspecific (siNS) or OGT (siOGT) followed by glucose starvation for indicated hours. (**B**) Representative image of immunocytochemistry after knockdown of nonspecific (siNS) or endogenous OGT (siOGT) (red) and overexpression of GFP-LC3 (green) for quantification of LC3 puncta in H1299 cells. Nuclei visualized by DAPI staining (blue). Similar results were obtained in three independent experiments performed using the same conditions. Scale bar, 10 μm. *P* value is calculated by *t*-test (***p<0.0001). Data are expressed as mean ± SEM. (**C**) Representative image of immunocytochemistry after knockdown of endogenous ULK1 (siULK1) and reconstitution with WT (WT^R) or T754N ($T754N^R$) siRNA-resistant ULK1 in H1299 cells. All cells were glucose starved to induce autophagy. Treatment of cells with either vehicle or 40 nM of bafilomycin A_1 for 2 hours was done before fixation. Similar results were obtained in three independent experiments performed using the same conditions. Scale bar, 10 μm. *P* value is calculated by one-way ANOVA (***p<0.0001). Data are expressed as mean ± SEM. Immunoblot showing knockdown and reconstitution efficiency of ULK1 WT or T754N mutant in H1299 cells in parallel with the immunocytochemistry experiment.

Dephosphorylation and O-GlcNAcylation on ULK1 occur sequentially

A previous study has quantified phosphorylation dynamics on 711 phospho-peptides through high throughput mass spectrometric analyses (Wang et al., 2008). Elevated O-GlcNAcylation resulted in reduced phosphorylation on 280 sites and caused increased phosphorylation on 148 sites. The crosstalk or interplay between these two abundant modifications may have arisen both by steric competition for occupancy at the same or proximal sites and by each modification regulating the other's enzymatic machinery. Therefore, I decided to examine whether this crosstalk between O-GlcNAcylation and phosphorylation applies to ULK1, since it has been reported that ULK1 is phosphorylated by mTOR on S757 in nutrient rich conditions (Hwang et al., 2017; Kim et al., 2011). S757 is only three amino acids away from the O-GlcNAcylation site, and this phosphorylation is known to be significantly diminished during nutrient starvation (Kim et al., 2011). I observed dephosphorylation of ULK1 on S757 simultaneously occurring with O-GlcNAcylation on T754 (Fig. II-5A), indicating that these two different modifications may be able to crosstalk with each other. I also noticed that binding between ULK1 and mTOR decreased over the time course of starvation (Fig. II-5B).

Based on the preceding evidence, I set out to test whether there is a correlation between O-GlcNAcylation and phosphorylation on ULK1. ULK1 phosphorylation by mTOR is known to negatively regulate ULK1 activity when sufficient nutrients are available. Therefore, I treated cells with Torin1 to inhibit mTOR activity and found that ULK1 phosphorylation by mTOR on S757 decreased as O-GlcNAcylation on T754

increased (Fig. II-5C). Next, I reasoned that overexpression of constitutively active form of mTOR would sufficiently reverse O-GlcNAcylation during glucose starvation in order for this negative correlation to be valid. The constitutively active mutant of mTOR (mTOR CA) has its four sites mutated (I2017T, V2198A, L2216H, and L2260P) (Das et al., 2011). Using mTOR CA, I verified O-GlcNAcylation of ULK1 being reversed by overexpression of this mutant. ULK1 O-GlcNAcylation was dose-dependently decreased, while adjacent phosphorylation dose-dependently increased by mTOR CA overexpression (Fig. II-5D), indicating the reversible and alternative interplay between ULK1 O-GlcNAcylation and mTOR-dependent phosphorylation. In addition, WT and mutant forms of ULK1 were tested for O-GlcNAcylation and phosphorylation after glucose starvation was given. As expected, both T754N mutant and S757D (phospho-S757 mimic) mutant failed to obtain O-GlcNAcylation while both WT and S757A were capable of being O-GlcNAcylated (Fig. II-5E). These results provide evidence for consecutive dephosphorylation and O-GlcNAcylation. In other words, O-GlcNAcylation occurs after ULK1 phosphorylation on S757 is significantly diminished.

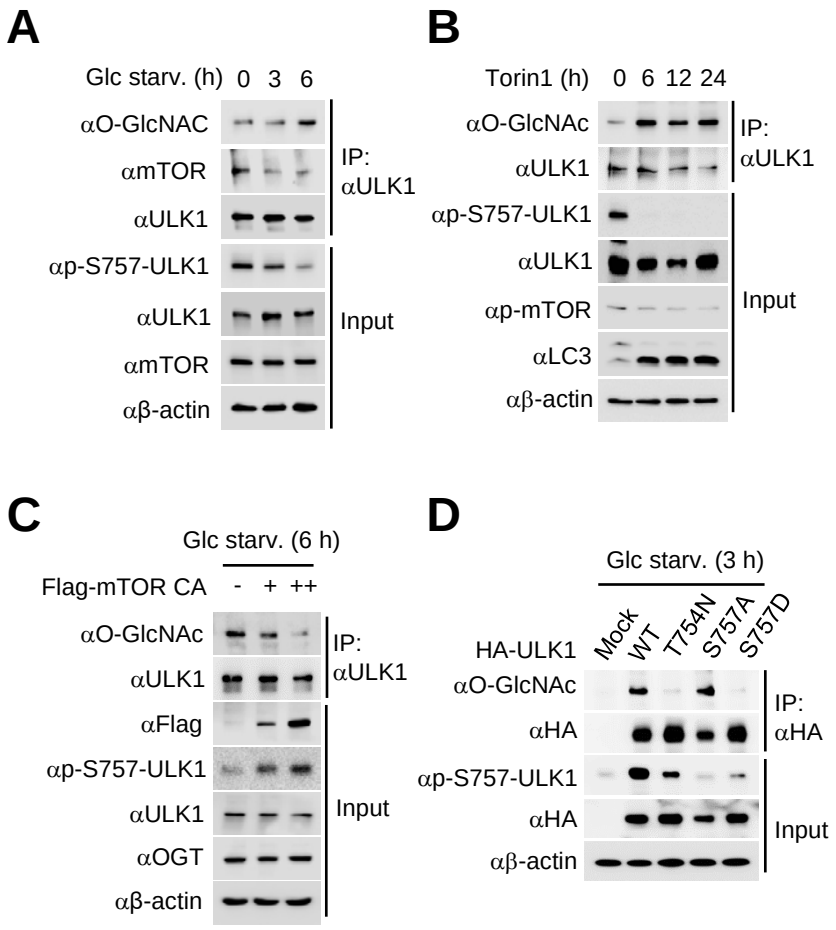

Figure II-5. Dephosphorylation and O-GlcNAcylation on ULK1 occur sequentially (**A**) Detection of ULK1 T754 O-GlcNAcylation and S757 phosphorylation after indicated hours of glucose starvation in H1299 cells. (**B**) Detection of ULK1 O-GlcNAcylation and S757 phosphorylation after treatment of H1299 cells with mTOR inhibitor Torin1 for indicated hours. (**C**) Overexpression of mTOR constitutively active mutant (mTOR CA) followed by detection of ULK1 O-GlcNAcylation. Cells were glucose-starved for 6 hours to induce ULK1 O-GlcNAcylation before harvest. (**D**) Overexpression of HA-tagged ULK1 WT and mutants T754N, S757A, and S757D in HEK293 cells, followed by glucose starvation, immunoprecipitation using anti-HA antibody, and immunoblot analysis against indicated antibodies.

PP1 is responsible for dephosphorylating S757 site during glucose starvation

Next, I predicted that there would be an active phosphatase responsible for dephosphorylation of ULK1. I found PP1 to be the case, whose interaction with ULK1 was significantly stronger than other phosphatases such as PP2A and PP5 during glucose starvation (Fig. II-6A). Moreover, PP5 knockdown resulted in increased LC3 II levels in contrast to PP1, supporting that PP1, but not PP5, would be a strong candidate phosphatase (Fig. II-6B). Although its total protein levels remained stable, PP1 showed increased binding to ULK1 during glucose starvation (Fig. II-6C). As the binding increased, ULK1 phosphorylation on S757 decreased, indicating a possible involvement of PP1 in mediating dephosphorylation of ULK1 on S757. Further, the interaction between ULK1 and PP1 was visualized by immunocytochemistry. Under nutrient rich conditions, ULK1 and PP1 did not colocalize in the cells, whereas during glucose starvation, their colocalization was significantly increased (Fig. II-6D).

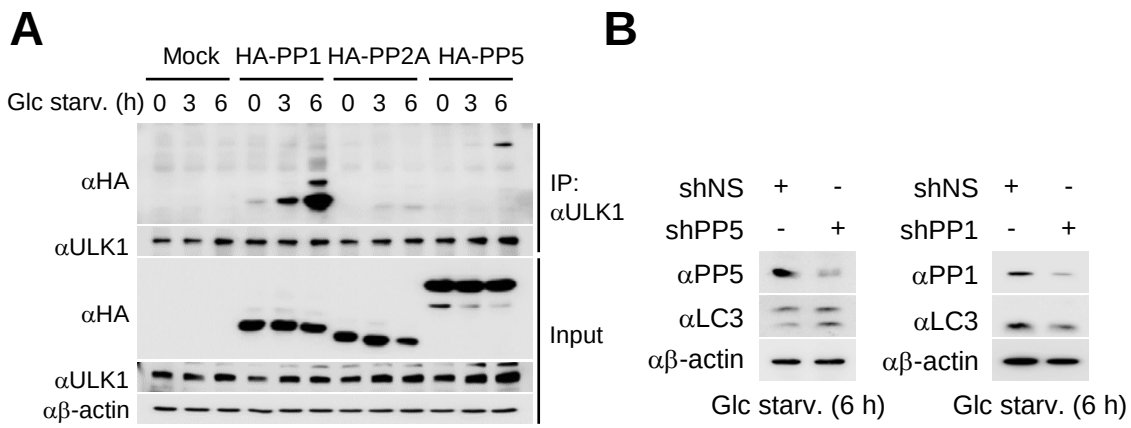
A
Mock
HA-PP1
HA-PP2A
HA-PP5
Glc starv. (h) 0 3 6 0 3 6 0 3 6 0 3 6
αHA
αULK1
IP: αULK1
αHA
αULK1
αβ-actin
Input
B
shNS + -
shPP5 - +
αPP5
αLC3
αβ-actin
Glc starv. (6 h)
shNS + -
shPP1 - +
αPP1
αLC3
αβ-actin
Glc starv. (6 h)

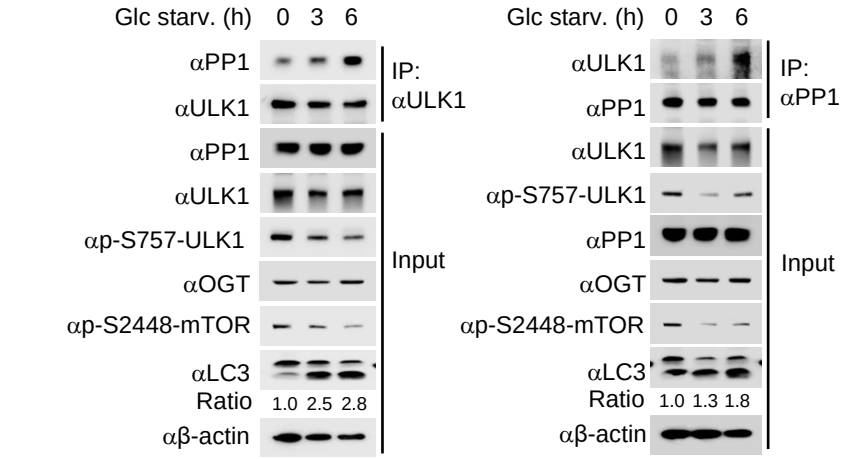
C
Glc starv. (h) 0 3 6
αPP1
αULK1
IP: αULK1
αPP1
αULK1
αp-S757-ULK1
αOGT
αp-S2448-mTOR
αLC3
Ratio 1.0 2.5 2.8
αβ-actin
Input
Glc starv. (h) 0 3 6
αULK1
αPP1
IP: αPP1
αULK1
αp-S757-ULK1
αPP1
αOGT
αp-S2448-mTOR
αLC3
Ratio 1.0 1.3 1.8
αβ-actin
Input

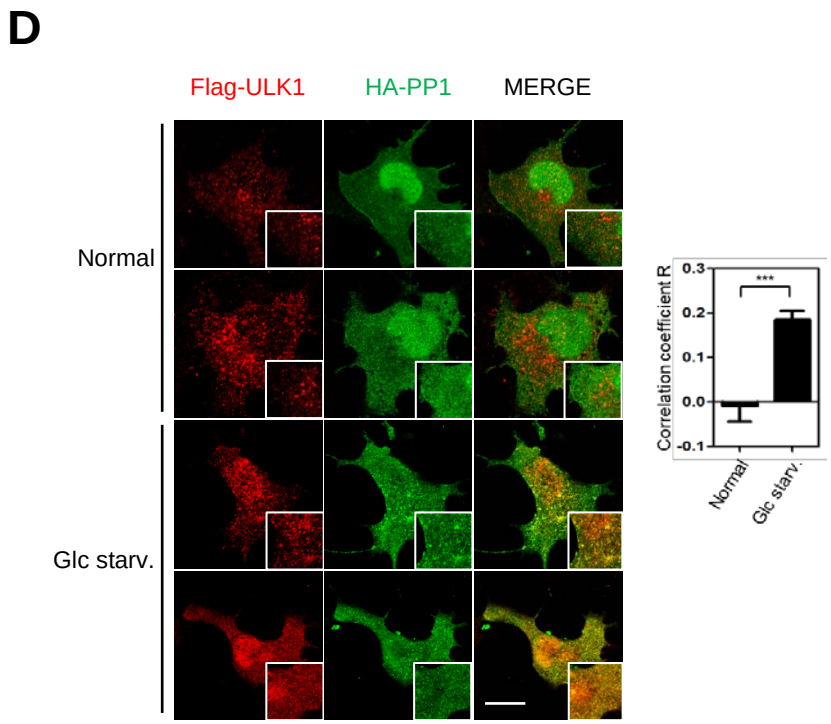

Figure II-6. PP1 is responsible for dephosphorylating S757 site during glucose starvation

(**A**) Comparison of binding between ULK1 and phosphatases (PP1, PP2A, and PP5) during glucose starvation in HEK293 cells. (**B**) PP5 knockdown results in increased LC3 II levels. HEK293 cells were transduced with either Non-Specific, PP5, or PP1 shRNA, glucose starved for 6 hours, and immunoblotted for detection of PP5, PP1, and LC3. (**C**) Co-immunoprecipitation of endogenous ULK1 and PP1 after indicated hours of glucose starvation in H1299 cells. The LC3-II/β-actin ratio is indicated. (**D**) Representative images of ULK1 and PP1 colocalization. H1299 cells were transfected with Flag-ULK1 and HA-PP1 and their colocalization was visualized using immunocytochemistry. Correlation coefficient R was calculated using ZEN program (ZEISS). Similar results were obtained in three independent experiments performed using the same conditions. Scale bar, 10 μm. *P* value is calculated by one-way ANOVA (***p<0.0001). Data are expressed as mean ± SEM.

Dephosphorylation event by PP1 is pivotal for proper interaction between ULK1 and OGT

Following the observation that ULK1 and PP1 colocalize, PP1 was knocked down to test whether PP1 is essential for ULK1 O-GlcNAcylation to occur. Indeed, the absence of PP1 led to dramatic decrease in ULK1 O-GlcNAcylation during glucose starvation (Fig. II-7A). Next, I determined whether this dephosphorylation event occurs specifically by PP1 by using a PP1 specific inhibitor, Tautomycetin. Treatment of glucose starved cells with Tautomycetin resulted in significantly reduced ULK1 O-GlcNAcylation (Fig. II-7B), indicating that dephosphorylation event is required for O-GlcNAcylation to occur. In addition, PP1 overexpression increased binding between ULK1 and OGT (Fig. II-7C). Also, ULK1 O-GlcNAcylation increased dose-dependently by overexpression of PP1, while adjacent phosphorylation was dramatically decreased (Fig. II-7D), indicating that dephosphorylation event by PP1 precedes binding between ULK1 and OGT and subsequent ULK1 O-GlcNAcylation. These results provided further evidence that withdrawal of mTOR from ULK1 during glucose starvation is not sufficient for ULK1 O-GlcNAcylation and that an active dephosphorylation event by PP1 is pivotal for proper interaction between ULK1 and OGT and subsequent O-GlcNAcylation. Also, overexpression of PP1 was sufficient to overcome suppression of ULK1 O-GlcNAcylation by mTOR, as was indicated by reversed O-GlcNAcylation and phosphorylation states (Fig. II-7E). Based on these results, I predicted that knockdown of endogenous PP1 would inhibit autophagosome formation in parallel with knockdown of endogenous OGT as shown earlier. As expected,

knockdown of PP1 resulted in the dramatically reduced number of GFP-LC3 puncta during glucose starvation (Fig. II-7F).

In sum, these data not only represent the close relationship between ULK1 and PP1 but also indicate that PP1 colocalizes with ULK1 to ensure that ULK1 stays dephosphorylated throughout starvation, possibly serving as a gatekeeper between O-GlcNAcylation by OGT and phosphorylation by mTOR.

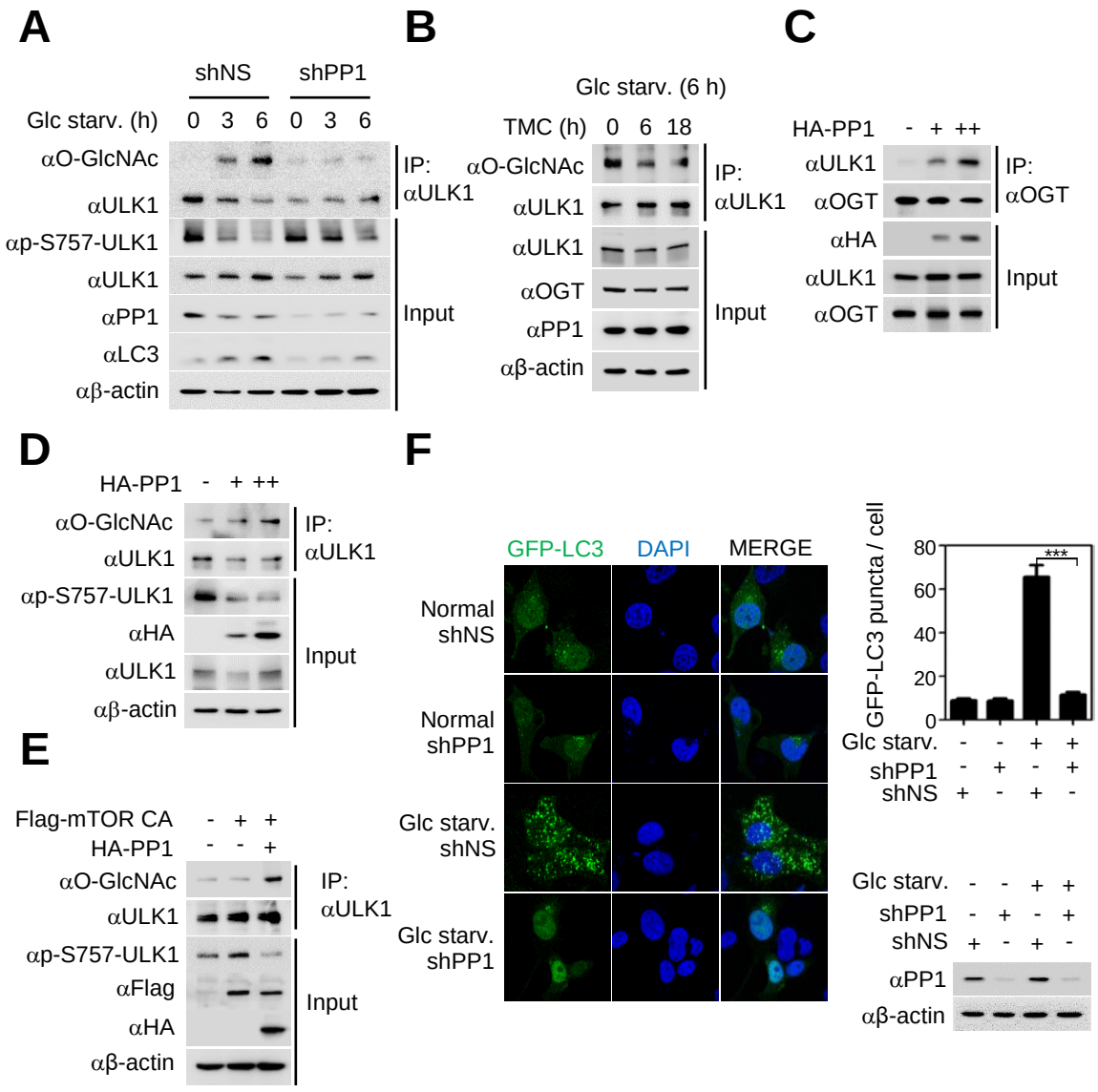
A
shNS
shPP1
Glc starv. (h) 0 3 6 0 3 6
αO-GlcNAc
αULK1
IP: αULK1
αp-S757-ULK1
αULK1
αPP1
αLC3
αβ-actin
Input
B
Glc starv. (6 h)
TMC (h) 0 6 18
αO-GlcNAc
αULK1
IP: αULK1
αULK1
αOGT
αPP1
αβ-actin
Input
C
HA-PP1 - + ++
αULK1
αOGT
IP: αOGT
αHA
αULK1
αOGT
Input
D
HA-PP1 - + ++
αO-GlcNAc
αULK1
IP: αULK1
αp-S757-ULK1
αHA
αULK1
αβ-actin
Input
E
Flag-mTOR CA - + +
HA-PP1 - - +
αO-GlcNAc
αULK1
IP: αULK1
αp-S757-ULK1
αFlag
αHA
αβ-actin
Input
F
GFP-LC3
DAPI
MERGE
Normal shNS
Normal shPP1
Glc starv. shNS
Glc starv. shPP1
GFP-LC3 puncta / cell
80
60
40
20
0
***
Glc starv. - - + +
shPP1 - + - +
shNS + - + -
Glc starv. - - + +
shPP1 - + - +
shNS + - + -
αPP1
αβ-actin

Figure II-7. Dephosphorylation event by PP1 is pivotal for proper interaction between ULK1 and OGT

(**A)** Immunoprecipitation assay detecting ULK1 O-GlcNAcylation in H1299 cells when PP1 was knocked down using shRNA and given glucose starvation for the indicated hours. (**B**) Tautomycetin treatment (10 nM) for the indicated hours followed by detection of ULK1 O-GlcNAcylation in H1299 cells. (**C**) Co-immunoprecipitation of ULK1 and OGT after overexpression of PP1 in HEK293 cells. (**D**) Overexpression of PP1 followed by detection of ULK1 O-GlcNAcylation and S757 phosphorylation in H1299 cells. (**E**) Detection of ULK1 O-GlcNAcylation and S757 phosphorylation when mTOR CA is expressed in the absence or presence of PP1 in H1299 cells. (**F**) Representative image of immunocytochemistry showing GFP-LC3 (green) puncta in H1299 cells with or without endogenous PP1 knockdown using shRNA. Nuclei visualized by DAPI staining (blue). Similar results were obtained in three independent experiments performed using the same conditions. Scale bar, 10 μm. *P* value is calculated by t-test (***$p<0.0001$). Data are expressed as mean ± SEM. Immunoblot analysis showing knockdown efficiency of endogenous PP1 in parallel with the immunocytochemistry experiment.

II-4. Discussion

In this study, I found previously predicted yet never identified crosstalk between O-GlcNAcylation and dephosphorylation mediated by PP1 governing ULK1 function during autophagy initiation. I addressed how a phosphatase can mediate O-GlcNAcylation, by demonstrating that PP1 dephosphorylates ULK1 on S757 which is in close vicinity with O-GlcNAcylation site T754. This may serve as a "priming event" for O-GlcNAcylation to occur during glucose starvation, and also may serve as an intermediary step between phosphorylation by mTOR and O-GlcNAcylation by OGT. Likewise, I speculate that there may be other common targets of PP1 and OGT during glucose starvation, since it has been reported that during glucose starvation global O-GlcNAcylation levels rise in H1299 cells (Yi et al., 2012).

Furthermore, this study indicates that a series of post-translational modification of ULK1 serves as a gatekeeper between pro-autophagic and anti-autophagic response, which is required for decision making process during autophagy occurrence. I speculate that since autophagy is an energy consuming process involving both short-term and long-term measures for cell survival, the cell may use a series of steps as checkpoints for determining whether the rest of the reactions should follow or not. My data highlight the newly identified regulation of autophagy by crosstalk between dephosphorylation and O-GlcNAcylation during the initial stages of autophagy, offering new therapeutic targets for autophagy-related diseases.

II-5. Materials and methods

Cell culture

HEK293, H1299, and SW620 cell lines were cultured in DMEM (Welgene, South Korea, LM001-05) or RPMI1640 (Welgene, South Korea, LM011-01) supplemented with 10 % (v/v) fetal bovine serum (Gibco, 26140-079), 100 U/ml penicillin and 100 μg/ml streptomycin (Welgene, South Korea, LS-20301). All cell lines used were regularly tested for mycoplasma contamination. Lipofectamine 3000 (Life Technologies, 100022052) and Gene In (Global Stem, catalog# 73802, 73012) transfection reagents were used and transfection was performed according to the manufacturers' protocol. Cells were harvested 24 to 36 h post-transfection. Experiments were performed under normal growth conditions, unless otherwise stated. For starvation, cells were washed twice in phosphate-buffered saline (Welgene, South Korea, LB001-02) and incubated in glucose-free DMEM (Welgene, South Korea, LM001-56) or RPMI1640 (Welgene, South Korea, LM011-60) supplemented with dialyzed fetal bovine serum (TCB, 101DI) for indicated hours.

Generation of *ULK1*$^{-/-}$ cells using CRISPR/Cas9

To generate KO cells, cells were transfected with px330 plasmid having following sequence: ULK1 Fw-5'-AGCAGATCGCGGGCGCCATG-3', Rv-5'-CATGGCGCCCGCGATCTGCT-3'. After transfection, single cells were grown until

colonies form. KO cells were selected based on protein expression and genomic DNA sequencing.

LC-ETD-MS/MS analysis

Flag-tagged ULK1 was coexpressed with OGT to induce O-GlcNAcylation. ULK1 was immunopurified using M2 beads, washed and eluted. The protein was denatured with 8 M urea in 50 mM ammonium bicarbonate (ABC) and followed by reduction and alkylation of cysteine thiols. After dilution to 1 M urea concentration with 50 mM ABC buffer, protein digestion by trypsin was performed at 37 °C for overnight. SPE clean up and sample concentration in speed-vac was preceded before mass spec analysis. LC-ETD-MS/MS experiment was performed on Orbitrap Fusion Lumos mass spectrometry (Thermo Fisher Scientific) coupled with nanoACQUITY UPLC (Waters) equipped with an in-house packed capillary analytical column (75 μm x 100 cm) and trap column (150 μm x 3 cm) with 3 μm Jupiter C18 particles (Phenomenex). The acquired ETD-MS/MS dataset was searched by MS-GF+ algorithm at 10 ppm of precursor ion mass tolerance against the SwissProt Homo sapiens proteome database.

Plasmids

Px330 sgRNA cloning vector for generating CRISPR Cas9 KO for ULK1 was acquired from Addgene (#42230). Sequence for siULK1 has been described previously (Gao, 2011). Mutations were introduced using *n*Pfu-Forte mutagenesis kit (Enzynomics, P410).

Antibodies and reagents

Anti- LC3B antibody (NB100-2220) was purchased from Novus Biologicals. Anti-ULK1 antibody (A7481), anti-Flag antibody (F3165), anti-β-actin antibody (A1978) were from Sigma Aldrich; anti-PP1 antibody (sc-7482), anti-mTOR antibody (sc-1549-R) were from Santa Cruz Biotechnology; anti-O-linked N-acetylglucosamine RLII antibody (Ab2739), and anti-OGT antibody (Ab96718) were from Abcam; anti-p-S757 ULK1 antibody (#6888), anti-p-S2448 mTOR antibody (#2971S) were from Cell Signaling; anti-HA antibody (#MMS-101R) was from Covance; anti-PP5 antibody (A300-909A) was from Bethyl Laboratories; WGA beads (AL-1023S) were from Vector Laboratories; Torin 1 (4247) and tautomycetin (2305) were from Tocris.

Co-immunoprecipitation assays

All cells were briefly rinsed with ice-cold PBS before collection. Cells were lysed in EBC200 buffer (50 mM Tris-HCl [pH 8.0], 0.2 M NaCl, 0.5 % NP-40, and protease inhibitors) on ice for 30 min. The lysates were collected and cleared by centrifugation at 14,000 × g for 10 min at 4 °C. Total protein concentration in the lysates was determined using the Bio-Rad Protein Assay Dye Reagent Concentrate (Bio-Rad, #500-0006). For co-immunoprecipitation assays, lysates were immunoprecipitated with protein A- and protein G-sepharose beads (GE Healthcare) for 2-4 hours with indicated antibodies. The beads were pelleted and washed five times in EBC200 buffer and then resuspended in

SDS PAGE-loading buffer. Bound proteins were eluted by boiling, resolved by SDS-PAGE, followed by immunoblot analysis. The blots were blocked and incubated in PBS containing 3 % BSA and indicated antibody for 2-4 hours. After six 10-min washes in 0.1 % Triton X-100 in PBS (PBS-T), the blots were incubated in horse radish peroxidase-conjugated secondary antibody in PBS-T/ 3 % BSA for 1-2 hours. For detection of bound proteins, the blots were washed five times in PBS-T, and then incubated in ECL.

Immunofluorescence microscopy

Cells grown on coverslips at a density of 7×10^4 cells were washed three times with PBS and then fixed with 2 % paraformaldehyde in PBS for 10 min at room temperature. Fixed cells were permeabilized with PBS-T for 10 min at room temperature. Blocking was performed with 3 % bovine serum in PBS-T for 30 min. For staining, cells were incubated with indicated antibodies for 4 hours at room temperature, followed by incubation with fluorescent labelled secondary antibodies for 1 hour. The following fluorescent secondary antibodies were used: donkey anti-mouse IgG; AlexaFluor 488, AlexaFluor 594; donkey anti-rabbit IgG AlexaFluor 488, AlexaFluor 594 (all from Invitrogen). Cells were mounted and visualized under a confocal microscope (Zeiss, LSM700). For autophagy studies, cells were transfected with GFP-LC3/mCherry-GFP-LC3 and sub-cultured onto coverslips followed by glucose starvation and fixation. For co-localization studies, cells were transfected with HA-PP1/Flag-ULK1 and sub-cultured onto coverslips followed by glucose starvation and fixation. The following day,

cells were incubated with either complete media or glucose starvation media for indicated times.

In vitro OGT assay

Recombinant Flag-OGT protein purified from HEK293 cells and recombinant 6X His-tagged ULK1 protein purified from *E. coli* were mixed in the reaction buffer (50 mM Tris-HCl pH 7.5, 12.5 mM $MgCl_2$, 2 mM UDP-GlcNAc, 1 mM DTT) in a final volume of 25 µl per sample. The samples were incubated at 37ºC for 24 hours. The reaction was resolved with SDS-PAGE, blotted onto a polyvinylidene difluoride (PVDF) membrane, followed by immunoblotting with anti-O-GlcNAc antibody to detect O-GlcNAcylation of ULK1.

Statistical analysis

All experiments were performed independently at least three times. Values are expressed as mean ± s.e.m. Significance was analyzed using one-tailed, unpaired *t*-test or one-way ANOVA. $P<0.05$ was considered statistically significant. *p < 0.01, **p < 0.001, ***p < 0.0001.

CHAPTER III.

ULK1 O-GlcNAcylation is crucial for activating VPS34 via ATG14L during autophagy initiation

III-1. Summary

Here, I provide evidence that ULK1 O-GlcNAcylation is crucial for the proper activation of VPS34 via ATG14L, the step which is essential for PI(3)P production and phagophore formation and subsequent autophagy initiation.

O-GlcNAcylation mutants T754N and T754A exhibited little or no change of kinase activity on ATG13. Also, the O-GlcNAc mutants had no significant defects in the ability to bind ATG13. Next, I investigated on the binding affinity of ULK1 with early players of autophagy such as ATG14L and VPS34 in the absence of glucose. I observed that ATG14L binding to ULK1 O-GlcNAcylation mutants T754N and T754Q was dramatically decreased when compared to ULK1 WT. In addition, ATG14L exhibited diminished binding with ULK1 when OGT was knocked down. Conversely, OGT WT, but not the mutant, caused increased binding between ULK1 and ATG14L. Moreover, when mTOR CA mutant was overexpressed, ULK1-ATG14L binding decreased as opposed to increased S757 phosphorylation. Moreover, the regulation of interaction between ULK1 and ATG14L was unique to ULK1 O-GlcNAcylation.

Based on the previous studies showing that AMPK and mTORC1 is antagonistic to each other on the function of ULK1, I investigated on where O-GlcNAcylation fits into the process. Through AMPK inhibition and AMPK knockdown experiments, I discovered that ULK1 O-GlcNAcylation occurs after AMPK-dependent phosphorylation.

ATG14L was phosphorylated by ULK1 *in vitro*. Moreover, using *in vitro* lipid kinase assays, I observed the failure of ULK1-ATG14L binding resulting in the failure of VPS34 lipid kinase activation. Given that WIPI puncta are dependent on VPS34 activity and PI3P, WIPI puncta formation was compared between ULK1 WT and T754N-reconstituted cells. When given glucose starvation, ULK1 T754N-reconstituted cells exhibited significantly less WIPI puncta than did ULK1 WT-reconstituted cells. Together, these data highlight that ULK1 O-GlcNAcylation is important for induction of VPS34 lipid kinase activity by ATG14L, which is critical for PI(3)P conversion and phagophore formation.

III-2. Introduction

Autophagy initiation is regulated by ULK1, which functions as a serine/threonine kinase and is mainly present in the cytosolic organelles such as ER, lysosome, mitochondria as well as cytosol. The formation of the ULK1, Atg13, and FIP200 complex is not altered by nutrient conditions nor mTOR signaling in mammals (Hosokawa et al., 2011; Shang, 2011). When activated, ULK1 phosphorylates Atg13 and FIP200, triggering complex activity in the initial steps of autophagosome biogenesis (Jung et al., 2009).

There are two major upstream regulators of ULK1: the mechanistic target of rapamycin complex 1 (mTORC1) and AMPK. mTORC1 is a protein complex consisting of mTOR serine/threonine kinase, Raptor, MLST8, PRAS40, and DEPTOR. It functions as an ATP- and amino acid-sensor to balance nutrient availability and cell growth and the activation of mTORC1 inhibits autophagy (Mizushima et al., 2010). Conversely, AMPK regulates cellular metabolism to maintain energy homeostasis and promotes autophagy. ULK1 is phosphorylated on serine 757 site by mTOR in nutrient rich conditions, inhibiting ULK1 activation via disrupting its binding to AMPK (Hosokawa et al., 2011; Mizushima et al., 2010). Upon glucose starvation, AMPK inhibits mTORC1 and phosphorylates ULK1 on S317 and S555 sites to activate it and consequently enable autophagy initiation. Thus, AMPK and mTORC1 regulate autophagy through coordinated phosphorylation of ULK1.

ULK1 regulates localization of a class III PI3 kinase called VPS34, which phosphorylates 3' position of the phosphatidylinositol to produce PI(3)P, a key molecular marker for intracellular trafficking and autophagosome formation (Backer, 2008; Hara et al., 2008; Itakura and Mizushima, 2010). VPS34 is the only PI3 kinase in yeast and is essential for protein sorting to the vacuole via the endolysosomal pathway by producing PI(3)P (Backer, 2016; Schu et al., 1993). PI(3)P is localized to the endosomal compartment and required for recruitment of downstream factors that contain PI(3)P-binding domains (Misra et al., 2001).

VPS34 exists in different complexes and is involved in a variety of cellular functions, such as multivesicular body pathway, retrograde trafficking from endosomes to the Golgi, phagosome maturation, and autophagy (Backer, 2008). It forms a stable complex with VPS15. VPS15 can also associate with Beclin1, which serves as a binding partner for several proteins which either promote (i.e. ATG14L, UVRAG, BIF1, and AMBRA-1) or inhibit (i.e. BCL2, BCLXL, and RUBICON) the autophagic function of VPS34 (Itakura et al., 2008; Liang et al., 2006; Matsunaga et al., 2009; Pattingre et al., 2008; Sun et al., 2008; Takahashi et al., 2008; Zalckvar et al., 2009; Zhong et al., 2009). In particular, ATG14L functions as a positive regulator of autophagosome formation because it determines the localization of VPS34 and the association with VPS34 complex is a prerequisite for the activation of VPS34 lipid kinase activity via AMPK (Kim et al., 2013; Matsunaga et al., 2009). However, little has been investigated on the mechanism of how ATG14L associates with VPS34-Belclin1 complex.

III-3. Results

ULK1 O-GlcNAcylation mutation had normal kinase activity and exhibited normal structural characteristics

Since T754 O-GlcNAcylation site is within the regulatory region of ULK1, this modification may alter its kinase activity. Therefore, I performed *in vitr*o kinase assay using ATG13 as a substrate, and found that T754N and T754A mutants exhibited little or no change of kinase activity on ATG13 (Fig. III-1A). In order to exclude the possibility that the mutation results in structural defects, I performed immunoprecipitation of WT and mutant ULK1 with ATG13. There was no significant defect in the ability to bind ATG13 (Fig. III-1B).

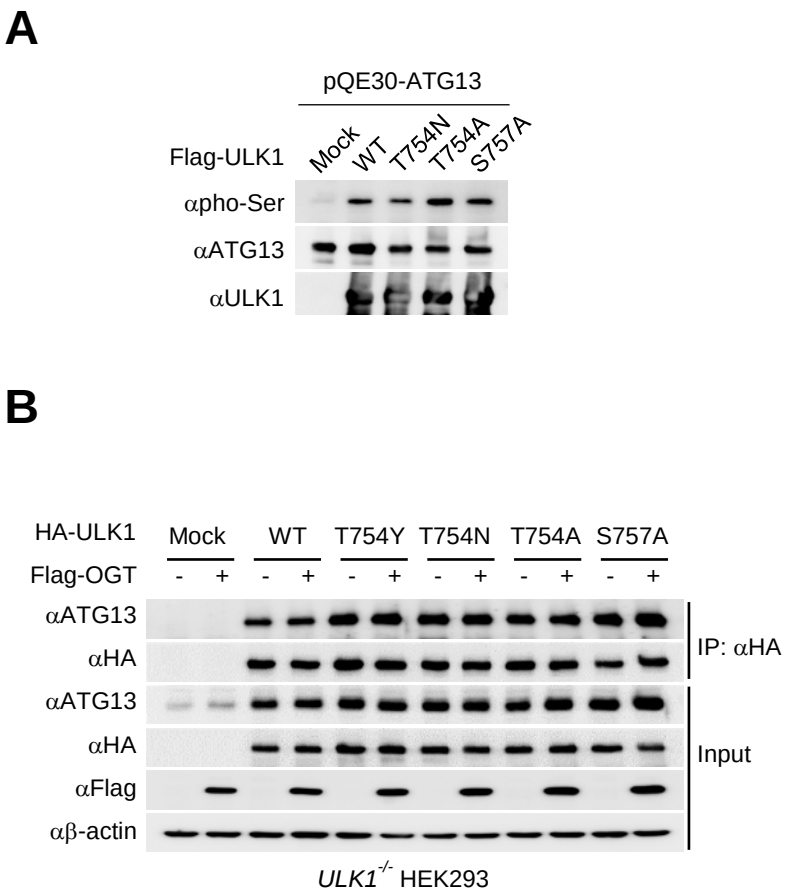

Figure III-1. ULK1 O-GlcNAcylation mutation had normal kinase activity and exhibited normal structural characteristics

(**A**) Flag M2 bead-pulled down Flag-ULK1 was purified from HEK293 cells after 3 hours of glucose starvation. ATG13 was cloned into pQE30 vector to be expressed in M15pRep *E. coli* cells. His-tagged ATG13 protein was purified using Ni-NTA beads and eluted for *in vitro* kinase assay. Phosphorylation of ATG13 was detected using monoclonal anti-phosphoserine antibody. See Experimental Procedures section for detailed protocol. (**B**) *ULK1*$^{-/-}$ HEK293 cells were transfected with HA-ULK1 WT, T754Y, T754N, T754A, or S757A and their binding affinity with ATG13 was tested in the absence or presence of OGT.

ULK1 O-GlcNACylation is essential for its interaction with ATG14L

I decided to explore other aspects of ULK1 function which would be affected by O-GlcNAcylation, such as protein-protein interaction. I tested the binding affinity with early players of autophagy such as ATG14L and VPS34. Being a positive regulator of autophagosome formation during autophagy and an important regulator of VPS34 complex, ATG14L binding to ULK1 T754N and T754Q was dramatically decreased when compared to ULK1 WT (Fig. III-2A). Intriguingly, knockdown of OGT significantly decreased the interaction between ULK1 and ATG14L (Fig. III-2B). This coincided with decreased LC3 II conversion, which was possibly due to the failure of ATG14L to bind ULK1. Based on my observation that ULK1 O-GlcNAcylation is required for proper binding to ATG14L, I examined whether overexpression of either WT or enzymatically dead mutant of OGT would alter the binding between ULK1 and ATG14L. As expected, OGT WT, but not the mutant, caused increased binding between ULK1 and ATG14L, confirming the importance of O-GlcNAcylation in facilitating their interaction (Fig. III-2C). In addition, since overexpression of mTOR CA led to decreased O-GlcNAcylation, I reasoned that this would also lead to reduced ULK1-ATG14L binding. Indeed, ULK1-ATG14L binding decreased as opposed to S757 phosphorylation which increased due to mTOR activity (Fig. III-2D).

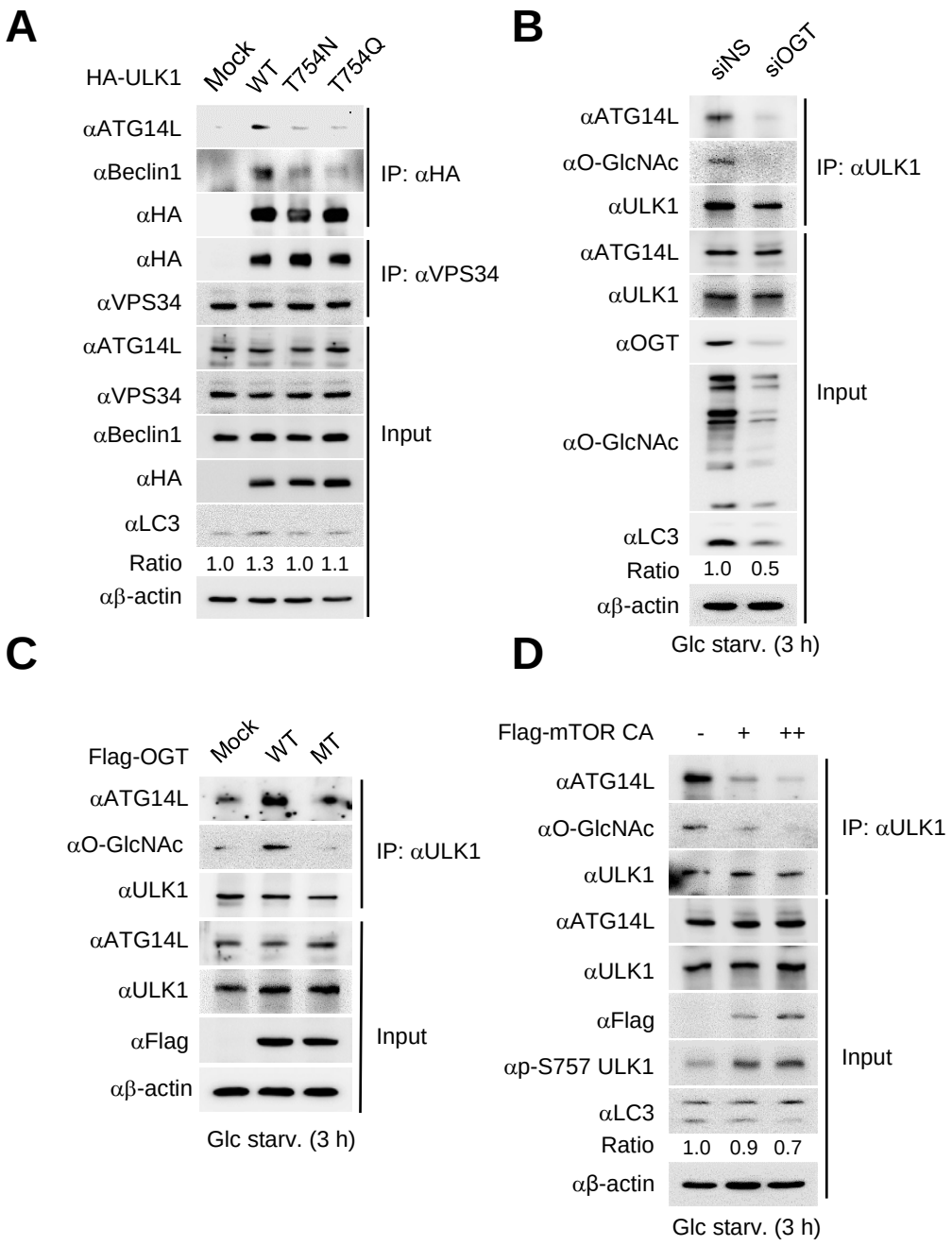
A
HA-ULK1
Mock
WT
T754N
T754Q
αATG14L
αBeclin1
αHA
IP: αHA
αHA
αVPS34
IP: αVPS34
αATG14L
αVPS34
αBeclin1
αHA
αLC3
Input
Ratio
1.0 1.3 1.0 1.1
αβ-actin
B
siNS
siOGT
αATG14L
αO-GlcNAc
αULK1
IP: αULK1
αATG14L
αULK1
αOGT
αO-GlcNAc
αLC3
Input
Ratio
1.0 0.5
αβ-actin
Glc starv. (3 h)
C
Flag-OGT
Mock
WT
MT
αATG14L
αO-GlcNAc
αULK1
IP: αULK1
αATG14L
αULK1
αFlag
αβ-actin
Input
Glc starv. (3 h)
D
Flag-mTOR CA
-
+
++
αATG14L
αO-GlcNAc
αULK1
IP: αULK1
αATG14L
αULK1
αFlag
αp-S757 ULK1
αLC3
Input
Ratio
1.0 0.9 0.7
αβ-actin
Glc starv. (3 h)

Figure III-2. ULK1 O-GlcNACylation is essential for its interaction with ATG14L
(**A**) Co-immunoprecipitation of ULK1 WT or T754N/T754Q mutants with endogenous ATG14L, Beclin1, and VPS34 in HEK293 cells after 3 hours of glucose starvation. Input was divided in half to perform two separate co-immunoprecipitation assays. The LC3-II/β-actin ratio is indicated. (**B**) Knockdown of endogenous OGT followed by 3 hours of glucose starvation and co-immunoprecipitation with anti-ULK1 antibody followed by immunoblot analysis with anti-ATG14L, anti-O-GlcNac, and ULK1 antibodies in H1299 cells. The LC3-II/β-actin ratio is indicated. (**C**) Co-immunoprecipitation of endogenous ULK1 and ATG14L when OGT WT or enzymatic dead mutant is overexpressed in HEK293 cells. (**D**) Overexpression of mTOR CA mutant in HEK293 cells upon glucose starvation for 3 hours. Co-immunoprecipitation assay was performed with anti-ULK1 antibody followed by immunoblot analysis using indicated antibodies. The LC3-II/β-actin ratio is indicated.

ATG14L binding function is unique to O-GlcNAcylation

One may argue the legitimacy of O-GlcNAcylation because dephosphorylation event might be sufficient to trigger the interaction between ULK1 and ATG14L. In order to test this possibility, I overexpressed PP1 to dephosphorylate ULK1 and then knocked down OGT so that ULK1 stays dephosphorylated and deO-GlcNAcylated. Surprisingly, the interaction between ULK1 and ATG14L diminished when OGT was knocked down, indicating that O-GlcNAcylation has its own function besides the crosstalk with the adjacent phosphorylation (Fig. III-3A). I continued to confirm the hypothesis by comparing ULK1 WT with O-GlcNAc mutants T754N and T754Q, phosphorylation mutant S757A, and double mutants T754N/S757A. T754N/S757A mutant was included because this form would represent dephosphorylated and deO-GlcNAcylated state of ULK1. Intriguingly, only WT and S757A mutant were able to bind ATG14L, indicating that dephosphorylated and deO-GlcNAcylated ULK1 showed attenuated binding to ATG14L (Fig. III-3B). In sum, O-GlcNAcylation requires dephosphorylation event yet it confers ULK1 its own function, which is the interaction with ATG14L.

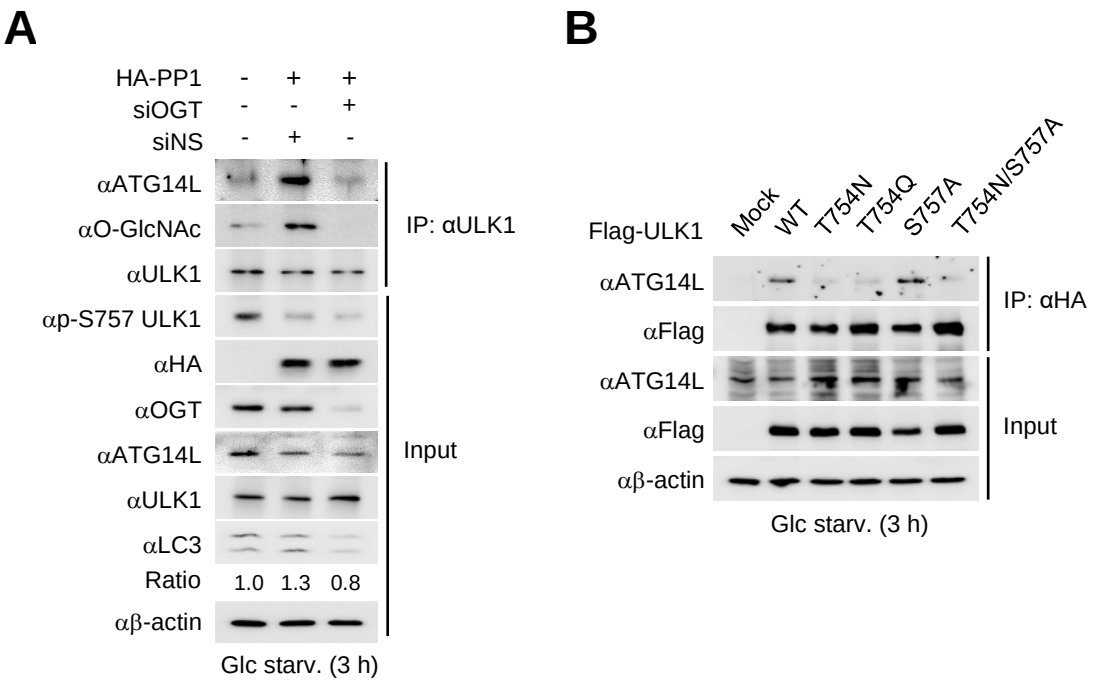

Figure III-3. ATG14L binding function is unique to ULK1 O-GlcNAcylation
(**A**) Overexpression of PP1 followed by knockdown of OGT in H1299 cells. Immunoprecipitation was performed using anti-ULK1 antibody followed by immunoblotting using indicated antibodies. Glucose starvation was given for 3 hours before harvest. (**B**) ULK1 WT, T754N, T754Q, S757A, and T754N/S757A mutants were reconstituted in *ULK1*$^{-/-}$ HEK293 cells. Glucose starvation was given for 3 hours before harvest.

Phosphorylation by AMPK precedes O-GlcNAcylation

Based on the previous studies showing that AMPK and mTORC1 is antagonistic to each other on the function of ULK1, I wondered where O-GlcNAcylation fits into the process. I treated cells with an AMPK inhibitor, Compound C, over the course of glucose starvation and observed dramatically decreased O-GlcNAcylation on ULK1 (Fig. III-4A). This result indicated that ULK1 O-GlcNAcylation occurs after AMPK phosphorylates ULK1 and this phosphorylation is required for O-GlcNAcylation to occur. To further verify this hypothesis, I transiently knocked down AMPKα using shRNA in glucose-starved cells. In parallel with Compound C experiment, AMPK knockdown also diminished ULK1 O-GlcNAcylation (Fig. III-4B). The effect of AMPK on ULK1 phosphorylation was detected by using antibody against p-S555 ULK1, which showed dramatic decrease when either Compound C or AMPK knockdown was applied. These data demonstrate that phosphorylation of ULK1 by AMPK precedes O-GlcNAcylation by OGT.

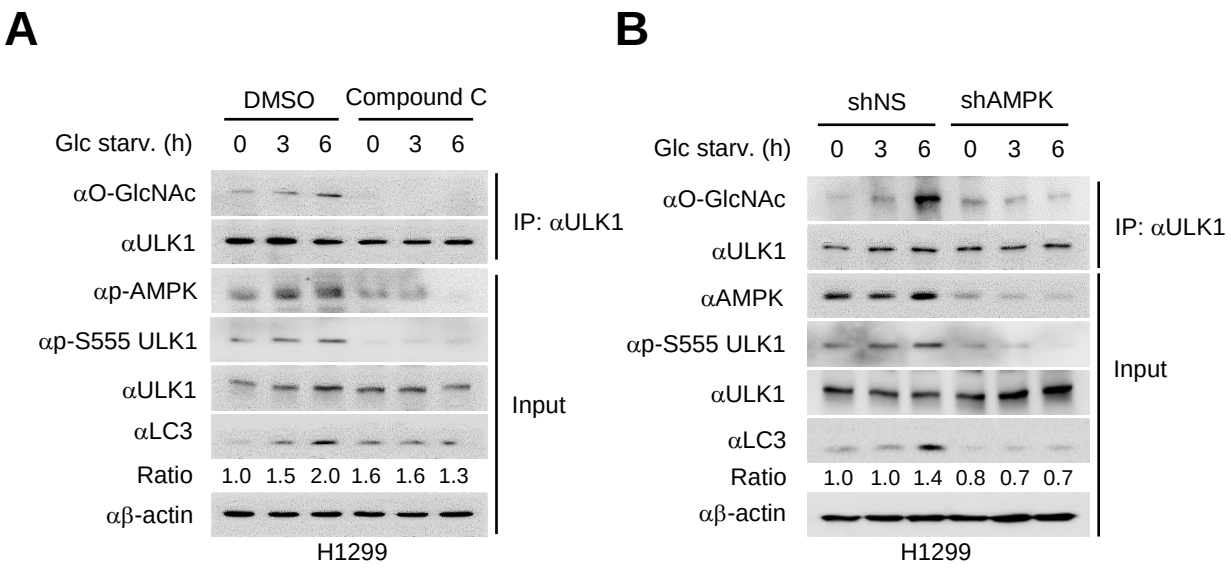

Figure III-4. Phosphorylation by AMPK precedes O-GlcNAcylation
(**A** and **B**) H1299 cells were treated with Compound C (10 μM) (**A**) or knocked down by AMPKα shRNA (**B**) during glucose starvation for the indicated hours. Immunoprecipitation was performed with anti-ULK1 antibody followed by immunoblot analysis using the indicated antibodies.

Interplay between dephosphorylation and O-GlcNAcylation of ULK1 governs autophagy initiation process

Since I have discovered that PP1 upregulates ULK1 O-GlcNAcylation and that O-GlcNAcylation is required for ULK1-ATG14L interaction, I tested whether the interaction between ATG14L and ULK1 is affected by dephosphorylation of ULK1 on S757 by PP1. Overexpression of PP1 increased the binding between ULK1 and ATG14L dose-dependently during glucose starvation (Fig. III-5A). Since ULK1 is a serine/threonine kinase and components of VPS34 complex such as VPS34 and Beclin1 are phosphorylated by ULK1, I hypothesized that the interaction between ULK1 and ATG14L would also induce phosphorylation of ATG14L. This possibility was in line with the previous report that ATG14L phosphorylation mimics nutrient deprivation by stimulating the kinase activity of the VPS34 complex and facilitates formation of phagophore and autophagosome (Park et al., 2016). In order to visualize phosphorylation of ATG14L by ULK1, *in vitro* kinase assay was performed. In this assay, phosphorylated form of ATG14L was detected by autoradiography and ULK1 phosphorylation was also detected since it has auto-kinase activity (Fig. III-5B). Therefore, using this method, I verified that ULK1 can induce phosphorylation of ATG14L.

It has been shown that in the presence of ATG14L, the VPS34 complex is activated by AMPK, whereas in the absence of ATG14L the VPS34 complex is inhibited by AMPK (Kim et al., 2013). Based on this information, I hypothesized that the failure of ULK1-ATG14L binding would result in the failure of VPS34 lipid kinase activation. *In vitro* VPS34 lipid kinase assay confirmed that reconstitution of *ULK1*$^{-/-}$ cells with

ULK1 WT, but not T754N mutant, induced VPS34 lipid kinase activity (Fig. III-5C). Another *in vitro* VPS34 lipid kinase assay was performed by overexpressing PP1 in HEK293 cells. VPS34 activity was dose-dependently induced, as shown by the increased level of ^{32}P-PI(3)P (Fig. III-5D).

Given that VPS34 can be involved in multiple, non-autophagy processes, we set out to further verify whether the ULK1 O-GlcNac mutant disrupts an autophagy-specific function of VPS34. Members of the human WD-repeat protein interacting with phosphoinositides (WIPI) family play an important role in recognizing PI(3)P at the phagophore, and hence function as autophagy-specific PI(3)P-binding effectors (Proikas-Cezanne et al., 2015). Since WIPI puncta are dependent on VPS34 activity and PI(3)P, WIPI puncta formation was compared between ULK1 WT and T754N-reconstituted cells. When given glucose starvation, ULK1 T754N-reconstituted cells exhibited significantly less WIPI puncta than did ULK1 WT-reconstituted cells (Fig. III-5E). This result indicates that VPS34 activity which is indicated by WIPI puncta formation depends on ULK1 O-GlcNAcylation. Together, these data highlight that ULK1 O-GlcNAcylation is important for induction of VPS34 lipid kinase activity by ATG14L, which is critical for PI(3)P conversion and phagophore formation.

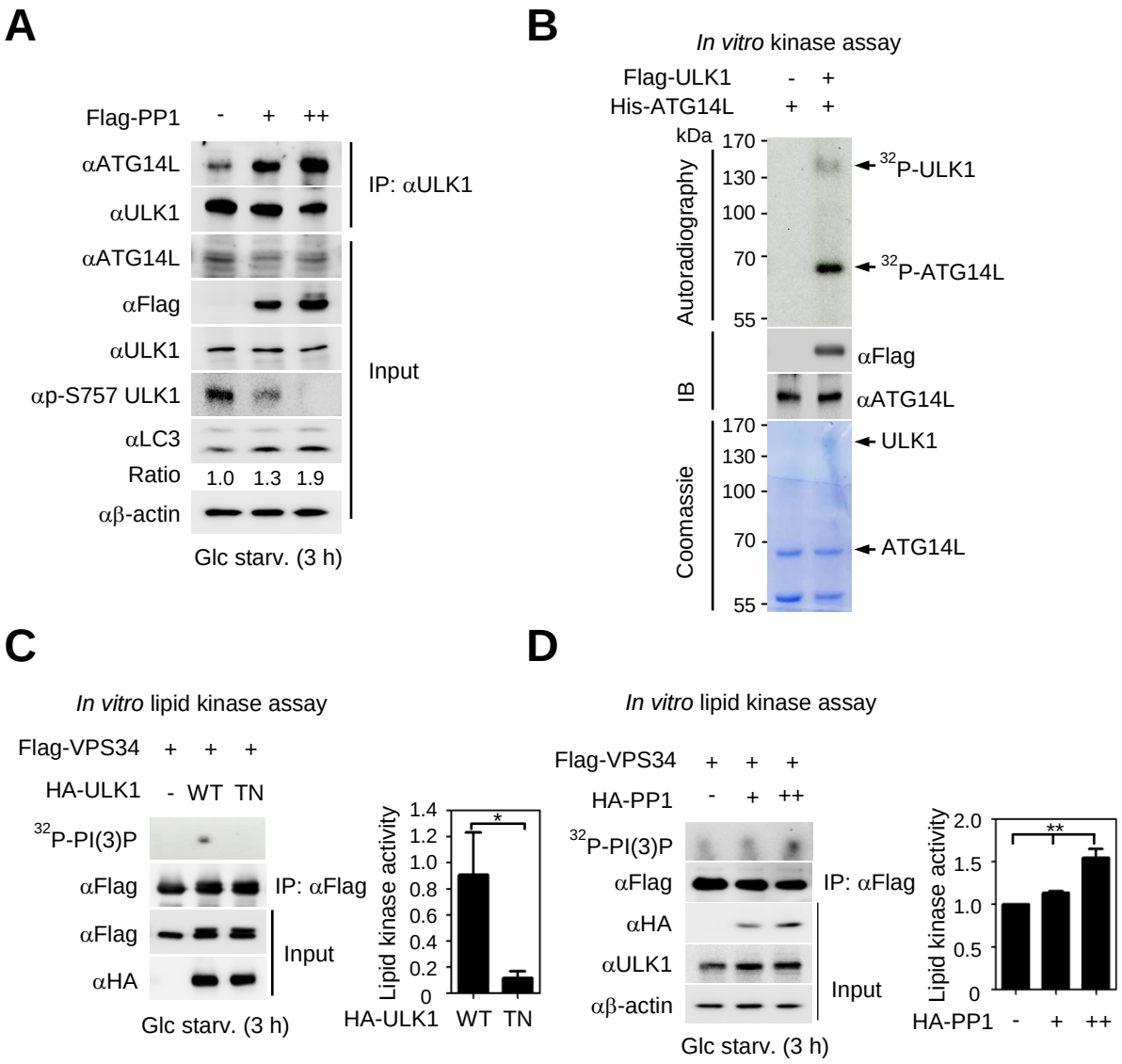
A
Flag-PP1 - + ++
αATG14L
αULK1
IP: αULK1
αATG14L
αFlag
αULK1
αp-S757 ULK1
αLC3
Input
Ratio 1.0 1.3 1.9
αβ-actin
Glc starv. (3 h)
B
In vitro kinase assay
Flag-ULK1 - +
His-ATG14L + +
kDa
170
130
100
70
55
Autoradiography
32P-ULK1
32P-ATG14L
IB
αFlag
αATG14L
Coomassie
ULK1
ATG14L
C
In vitro lipid kinase assay
Flag-VPS34 + + +
HA-ULK1 - WT TN
32P-PI(3)P
αFlag
IP: αFlag
αFlag
αHA
Input
Glc starv. (3 h)
Lipid kinase activity
1.4
1.2
1.0
0.8
0.6
0.4
0.2
0
*
HA-ULK1 WT TN
D
In vitro lipid kinase assay
Flag-VPS34 + + +
HA-PP1 - + ++
32P-PI(3)P
αFlag
IP: αFlag
αHA
αULK1
αβ-actin
Input
Glc starv. (3 h)
Lipid kinase activity
2.0
1.5
1.0
0.5
0
**
HA-PP1 - + ++

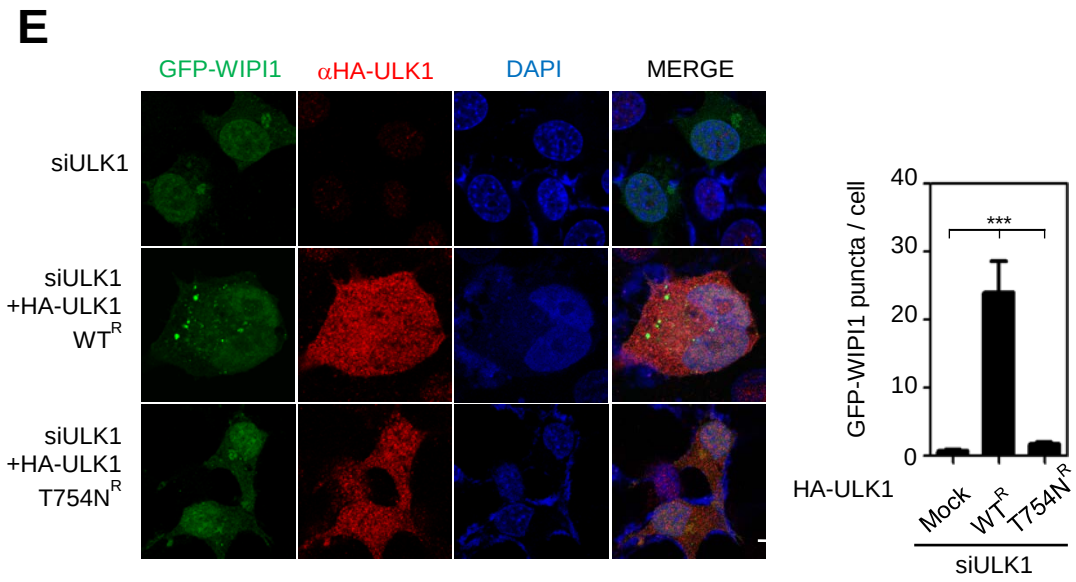

Figure III-5. Interplay between dephosphorylation and O-GlcNAcylation of ULK1 governs autophagy initiation process

(**A**) Overexpression of PP1 in H1299 cells upon glucose starvation for 3 hours. Co-immunoprecipitation was performed using anti-ULK1 antibody followed by immunoblot analysis with the indicated antibodies. (**B**) *In vitro* kinase assay. Flag-ULK1 overexpressing cells were glucose-starved for 3 hours and harvested for pull-down assay with anti-Flag M2 beads. The isolated protein was eluted with Flag peptide for *in vitro* kinase assay. *E. coli* strain M13 pREP was used for amplifying and purifying pQE-His-ATG14L protein by Ni-NTA pulldown. ^{32}P was used for detecting phosphorylation on ATG14L. (**C** and **D**) Lysates containing Flag-VPS34 were subjected to pull-down assay with anti-Flag M2 beads. The isolated protein was eluted with Flag peptide followed by *in vitro* lipid kinase assay. ^{32}P-PI(3)P production by VPS34 in response to ULK1 WT or T754N mutant overexpression (**C**) or PP1 overexpression (**D**) was measured using thin layer chromatography (TLC) followed by autoradiography. Three independent experiments were performed and were analyzed for statistics. *P* value is calculated by *t*-test (*p<0.01) or one-way ANOVA (**p<0.001). Data are expressed as mean ± SEM. (**E**) Representative images of immunocytochemistry after knockdown of endogenous ULK1 and reconstitution with WT (WT^R) or T754N (T754N^R) siRNA-resistant ULK1 in H1299 cells. Similar results were obtained in three independent experiments performed using the same conditions. Scale bar, 10 um. *P* value is calculated by one-way ANOVA (***p<0.0001). Data are mean ±SEM.

III-4. Discussion

In this study I demonstrated that ULK1 O-GlcNAcylation occurs after phosphorylation by AMPK. In addition, I exemplified how ULK1 O-GlcNAcylation is crucial for autophagosome formation by driving the lipid kinase activity of the VPS34 via ATG14L (Fig. III-6).

Previous studies have reported that OGT is recruited to sites of PI(3)P formation during growth factor signaling, suggesting that many signaling cascades triggered by PI3K are likely to be influenced by O-GlcNAcylation (Yang et al., 2008). By analogy from its recruitment to PI(3)P in the plasma membrane, OGT has been predicted to be directly recruited to the forming autophagosome (Hanover et al., 2010). I identified a specific target of OGT at the pre-autophagosomal structure, ULK1, whose localization to the phagophore recruits ATG14L to induce VPS34, a type III PI3K, and allows formation of PI(3)P. Generation of PI(3)P at the phagophore by VPS34 is a critical event during pre-autophagosomal structure formation. Two independent studies indicate that ATG14L positively regulates autophagy by promoting double-membrane formation during autophagy, and that ATG14L deficiency causes defects in autophagosome formation (Matsunaga et al., 2009; Zhong et al., 2009). Moreover, the activity of ATG14L-containing VPS34 complex is strongly dependent on ULK1, yet detailed regulatory mechanism has not been fully investigated. In this study, I provided first

evidence that ULK1 O-GlcNAcylation exerts its function by upregulating VPS34 lipid kinase activity via increased binding between ULK1 and ATG14L.

Combined with the results in Chapter II, these data indicate that a series of post-translational modification of ULK1 is utilized by the cells as checkpoints for determining whether the rest of the reactions should follow or not.

More importantly, the coordinated modification of ULK1 by mTOR, AMPK, and OGT may explain the necessity of signal integration in the cell, in order to carefully respond to the complex extracellular environment. Under conditions of glucose depletion and sufficient amino acids, it would be advantageous for cells to activate AMPK and alter cellular metabolism by phosphorylating metabolic enzymes to promote amino acid utilization for energy production. Although AMPK would suppress mTORC1, it is likely that mTORC1 would not be completely inhibited when amino acids are available. This means that phosphorylation of S757 on ULK1 would still remain to inhibit ULK1. Therefore, mTOR-dependent phosphorylation of S757 on ULK1 needs to be actively removed by PP1 as the cell decides to initiate autophagy. In this regard, ULK1 S757 dephosphorylation may serve as a barrier between mTOR-dependent phosphorylation and O-GlcNAcylation. These findings represent a significant step towards understating how major cellular nutrient sensors are integrated to fine-tune autophagic response. Future studies directed at discovering similar examples of regulatory hub in the later stages of autophagy will be essential to understand how the cells dynamically respond to their nutritional status.

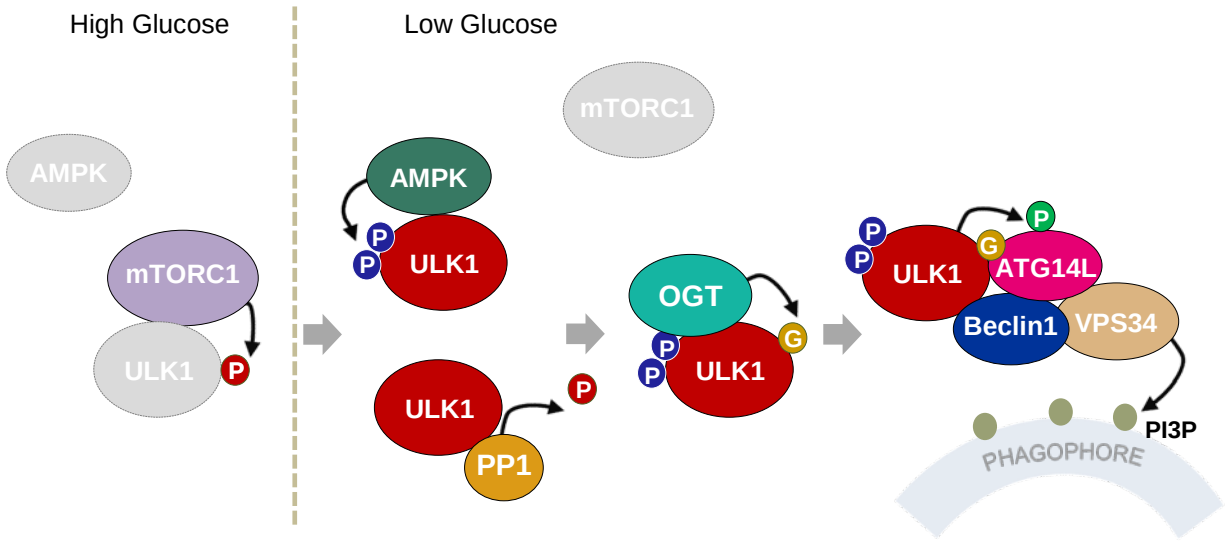

Figure III-6. A schematic model.
A combination of dephosphorylation by PP1, phosphorylation by AMPK, and O-GlcNAcylation by OGT on ULK1 during glucose starvation leads to the regulation of VPS34 activity via ATG14L and phagophore formation.

III-5. Materials and methods

Cell culture

HEK293, H1299, and SW620 cell lines were cultured in DMEM (Welgene, South Korea, LM001-05) or RPMI1640 (Welgene, South Korea, LM011-01) supplemented with 10 % (v/v) fetal bovine serum (Gibco, 26140-079), 100 U/ml penicillin and 100 μg/ml streptomycin (Welgene, South Korea, LS-20301). All cell lines used were regularly tested for mycoplasma contamination. Lipofectamine 3000 (Life Technologies, 100022052) and Gene In (Global Stem, catalog# 73802, 73012) transfection reagents were used and transfection was performed according to the manufacturers' protocol. Cells were harvested 24 to 36 h post-transfection. Experiments were performed under normal growth conditions, unless otherwise stated. For starvation, cells were washed twice in phosphate-buffered saline (Welgene, South Korea, LB001-02) and incubated in glucose-free DMEM (Welgene, South Korea, LM001-56) or RPMI1640 (Welgene, South Korea, LM011-60) supplemented with dialyzed fetal bovine serum (TCB, 101DI) for indicated hours.

Generation of *ULK1*$^{-/-}$ cells using CRISPR/Cas9

To generate KO cells, cells were transfected with px330 plasmids having following sequence: ULK1 #1 Fw-5'-AGCAGATCGCGGGCGCCATG-3', Rv-5'-

CATGGCGCCCGCGATCTGCT-3'. After transfection, single cells were grown until colonies form. KO cells were selected based on protein expression and genomic DNA sequencing.

Antibodies and reagents

Anti-Beclin1 antibody (NB110-87318) and anti-LC3B antibody (NB100-2220) were purchased from Novus Biologicals. Anti-ULK1 antibody (A7481), anti-Flag antibody (F3165), anti-ATG13 antibody (SAB4200100), anti-p-serine antibody (P5747), anti-β-actin antibody (A1978) were from Sigma Aldrich; anti-PP1 antibody (sc-7482), anti-mTOR antibody (sc-1549-R) were from Santa Cruz Biotechnology; anti-ATG14L antibody (Ab173943), anti-O-linked N-acetylglucosamine RLII antibody (Ab2739), and anti-OGT antibody (Ab96718) were from Abcam; anti-p-S757 ULK1 antibody (#6888), anti-p-S555 ULK1 antibody (#5869), anti-p-T172 AMPK antibody (#2531), anti-p-S2448 mTOR antibody (#2971S) and anti-VPS34 antibody (#3811S) were from Cell Signaling; anti-HA antibody (#MMS-101R) was from Covance; L-α-Phosphatidylinositol sodium salt (P0639) was from Sigma Aldrich; WGA beads (AL-1023S) were from Vector Laboratories; Torin 1 (4247) and tautomycetin (2305) were from Tocris.

Co-immunoprecipitation assays

All cells were briefly rinsed with ice-cold PBS before collection. Cells were lysed in EBC200 buffer (50 mM Tris-HCl [pH 8.0], 0.2 M NaCl, 0.5 % NP-40, and protease inhibitors) on ice for 30 min. The lysates were collected and cleared by centrifugation at 14,000 × g for 10 min at 4 °C. Total protein concentration in the lysates was determined using the Bio-Rad Protein Assay Dye Reagent Concentrate (Bio-Rad, #500-0006). For co-immunoprecipitation assays, lysates were immunoprecipitated with protein A- and protein G-sepharose beads (GE Healthcare) for 2-4 hours with indicated antibodies. The beads were pelleted and washed five times in EBC200 buffer and then resuspended in SDS PAGE-loading buffer. Bound proteins were eluted by boiling, resolved by SDS-PAGE, followed by immunoblot analysis. The blots were blocked and incubated in PBS containing 3 % BSA and indicated antibody for 2-4 hours. After six 10-min washes in 0.1 % Triton X-100 in PBS (PBS-T), the blots were incubated in horse radish peroxidase-conjugated secondary antibody in PBS-T/ 3 % BSA for 1-2 hours. For detection of bound proteins, the blots were washed five times in PBS-T, and then incubated in ECL.

***In vitro* kinase assay**

ULK1 proteins were immunoprecipitated from HEK293 cell with anti-Flag M2 agarose affinity gel (Sigma). The immune-complex was extensively washed with BC150 (20 mM Tris-HCL, pH 7.9, 15 % glycerol, 1 mM EDTA, 1mM DTT (dithiothreitol), 0.05 % NP40, and 150 mM KCl for three times, and with BC300 (same as BC150 except for 300 mM KCl) for three times, and lastly with BC150 for three times. Flag-peptide was

used for elution from the affinity gel. His-ATG14L proteins were purified from *E. coli* strain M15pRep using Ni-NTA resin (Qiagen). ULK1 and ATG14L proteins were incubated in kinase assay buffer containing 10 mM HEPES at pH 7.4, 50 mM NaCl, 10 mM $MgCl_2$, 10 mM $MnCl_2$, 1 mM DTT, protease inhibitors. 10 μM cold ATG and 10 μCi [γ-^{32}P]ATP were added per reaction. The kinase reaction was performed at 37 °C for 30 min and the reaction was terminated by adding SDS sample buffer and subjected to SDS–PAGE (polyacrylamide gel electrophoresis) and autoradiography.

***In vitro* VPS34 lipid kinase assay**

Flag-tagged VPS34-expressing HEK293 cells were immunoprecipitated with anti-Flag M2-agarose affinity gel as immunoprecipitation assay and washed with NP-40 buffer, eluted with 3X Flag peptide in TBS buffer (150 mM NaCl, 50 mM Tris-HCl [pH 7.4]). Immuno-purified complexes were equilibrated in kinase base buffer (20 mM HEPES [pH 7.4], 1 mM EGTA, 0.4 mM EDTA, and 5 mM $MgCl_2$) and then preincubated for 10 min at room temperature with 10 mM $MnCl_2$ and 2 μg sonicated phosphatidylinositol (Sigma). 10 μCi [γ-^{32}P] ATP and 1 mM cold ATP were added and incubated for 15 min at room temperature. The kinase reactions were stopped by directly adding 10 μl 1 M HCl, followed by lipid extraction with 2 volumes of methanol/$CHCl_3$ (1: 1). Samples were vortexed and centrifuged at maximum speed for 10 min. The organic phase was loaded on a thin-layer chromatography plate (Analtech). Resolution of phospho-lipid

was achieved using a buffer composition of $CHCl_3$/methanol/NH_4OH (30 %)/ water (129: 100: 4.29: 24). Resolved plates were analyzed by autoradiography.

Statistical analysis

All experiments were performed independently at least three times. Values are expressed as mean ± s.e.m. Significance was analyzed using one-tailed, unpaired *t*-test or one-way ANOVA. $P<0.05$ was considered statistically significant. *p < 0.01, **p < 0.001, ***p < 0.0001.

CONCLUSION

The activity of ATG14L-containing VPS34 complex is strongly dependent on ULK1, yet detailed regulatory mechanism has not been fully investigated until now. During my Ph. D course, I provided first evidence that ULK1 O-GlcNAcylation exerts its function by upregulating VPS34 lipid kinase activity via increased binding between ULK1 and ATG14L.

In addition, my research data indicate that a series of post-translational modification of ULK1 serves as a gatekeeper between pro-autophagic and anti-autophagic response, which is required for decision making process during autophagy occurrence. Since autophagy is an energy consuming process involving both short-term and long-term measures for cell survival, the cell may use a series of steps as checkpoints for determining whether the rest of the reactions should follow or not.

More importantly, I found previously predicted yet never exemplified crosstalk between O-GlcNAcylation mediated by OGT and dephosphorylation mediated by PP1 governing ULK1 function during autophagy initiation. I addressed how a phosphatase can mediate O-GlcNAcylation, by demonstrating that PP1 dephosphorylates ULK1 on S757 which is in close vicinity with O-GlcNAcylation site T754. This may serve as a "priming event" for O-GlcNAcylation to occur during glucose starvation, and also may serve as an intermediary step between phosphorylation by mTOR and O-GlcNAcylation by OGT. Also, because parts of PP1 complex has been reported to form a complex with

OGT, I speculate that there may be other common targets of PP1 and OGT during glucose starvation.

In line with these findings, it is notable that two independent studies have suggested that mTORC1 deactivation is an acute, active process and not merely a dampening of mTORC1 signaling due to dissipation of its upstream stimuli (Demetriades et al., 2014; Menon et al., 2014). This abrupt deactivation when no longer needed demonstrates that mTORC1 activity is tightly controlled and suggests a corresponding level of opposite control for mTORC1 downstream effectors such as the S6K, 4EBP, and ULK1 proteins. It is possible that PP1 not only serves as a mediator of crosstalk between O-GlcNAcylation and phosphorylation but also functions as a highly responsive antagonist of mTORC1 signaling pathway because it dephosphorylates one of the major downstream targets of mTORC1, which is ULK1.

The coordinated modification of ULK1 by three different nutrient sensors mTOR, AMPK, and OGT may explain the necessity of signal integration in the cell, in order to carefully respond to the complex extracellular and intracellular environment. Under conditions of glucose depletion and sufficient amino acids, it would be advantageous for cells to activate AMPK and alter cellular metabolism by phosphorylating metabolic enzymes to promote amino acid utilization for production of consumable forms of energy, such as ATP. Although AMPK would suppress mTOR during glucose starvation, it is likely that mTOR would not be completely inhibited when amino acids are available. This means that phosphorylation of S757 on ULK1 would still remain to inhibit ULK1 while the cell needs extra source of energy due to glucose

starvation. In order to overcome this dilemma, mTOR-dependent phosphorylation of S757 on ULK1 needs to be actively removed by PP1 as the cell decides to initiate autophagy.

In conclusion, my discoveries represent a significant step towards understating how major cellular nutrient sensors are integrated to fine-tune autophagic response. Future studies directed at discovering similar examples of regulatory hub in the later stages of autophagy will be essential to understand how the cells respond to their dynamic nutritional status.

REFERENCES

Alers, S., Löffler, A.S., Wesselborg, S., and Stork, B. (2012). Role of AMPK-mTOR-Ulk1/2 in the Regulation of Autophagy: Cross Talk, Shortcuts, and Feedbacks. Mol Cell Biol *32*, 2-11.

Arnold, C.S., Johnson, G.V.W., Cole, R.N., Dong, D.L.Y., Lee, M., and Hart, G.W. (1996). The Microtubule-associated Protein Tau Is Extensively Modified with O-linked N-acetylglucosamine. THE JOURNAL OF BIOLOGICAL CHEMISTRY *271*, 28741–28744.

Backer, J.M. (2008). The regulation and function of Class III PI3Ks: novel roles for Vps34. Biochemical Journal *410*, 1-17.

Backer, J.M. (2016). The intricate regulation and complex functions of the Class III phosphoinositide 3-kinase Vps34. Biochemical Journal *473*, 2251-2271.

Benjamin, D., and Hall, M.N. (2014). mTORC1: Turning Off Is Just as Important as Turning On. Cell *156*, 627-628.

Capra, M., Nuciforo, P.G., Confalonieri, S., Quarto, M., Bianchi, M., Nebuloni, M., Boldorini, R., Pallotti, F., Viale, G., Gishizky, M.L., *et al.* (2006). Frequent Alterations in the Expression of Serine/Threonine Kinases in Human Cancers. Cancer Research *66*, 8147-8154.

Chen, Q., Chen, Y., Bian, C., Fujiki, R., and Yu, X. (2013). TET2 promotes histone O-GlcNAcylation during gene transcription. Nature *493*, 561-564.

Cheng, X., Cole, R.N., Zaia, J., and Hart, G.W. (2000). Alternative O-Glycosylation/O-Phosphorylation of the Murine Estrogen Receptor B. Biochemistry *2000*, 11609-11620.

Cheng, X., and Hart, G.W. (2001). Alternative O-glycosylation/O-phosphorylation of serine-16 in murine estrogen receptor beta: Post-translational regulation of turnover and transactivation activity. Journal of Biological Chemistry *276*, 10570-10575.

Chou, C.F., Smith, A.J., and Omary, M.B. (1992). Characterization and Dynamics of 0-Linked Glycosylation of Human Cytokeratin 8 and 18. THE JOURNAL OF BIOLOGICAL CHEMISTRY *267*, 3901-3906.

Chou, T.Y., Hart, G.W., and Dang, C.V. (1995). c-Myc is glycosylated at threonine 58, a known phosphorylation site and a mutational hot spot in lymphomas. Journal of Biological Chemistry *270*, 18961-18965.

Chu, C.S., Lo, P.W., Yeh, Y.H., Hsu, P.H., Peng, S.H., Teng, Y.C., Kang, M.L., Wong, C.H., and Juan, L.J. (2014). O-GlcNAcylation regulates EZH2 protein stability and function. PNAS *111*, 1355-1360.

Cole, R.N., and Hart, G.W. (2001). Cytosolic O-glycosylation is abundant in nerve terminals. Journal of Neurochemistry *79*, 1080-1089.

Comer, F.I., and Hart, G.W. (2001). Reciprocity between O-GlcNAc and O-Phosphate on the Carboxyl Terminal Domain of RNA Polymerase II. Biochemistry *2001*, 7845-7852.

Das, F., Ghosh-Choudhury, N., Dey, N., Mandal, C.C., Mahimainathan, L., Kasinath, B.S., Abboud, H.E., and Choudhury, G.G. (2011). Unrestrained Mammalian Target of Rapamycin Complexes 1 and 2 Increase Expression of Phosphatase and Tensin Homolog Deleted on Chromosome 10 to Regulate Phosphorylation of Akt Kinase. Journal of Biological Chemistry *287*, 3808-3822.

Demetriades, C., Doumpas, N., and Teleman, A.A. (2014). Regulation of TORC1 in Response to Amino Acid Starvation via Lysosomal Recruitment of TSC2. Cell *156*, 786–799.

Dentin, R., Hedrick, S., Xie, J., Yates III, J., and Montminy, M. (2008). Hepatic Glucose Sensing via the CREB Coactivator CRTC2. Science *319*, 1402-1405.

Dong, D.L.Y., Xu, Z.S., Hart, G.W., and Cleveland, D.W. (1996). Cytoplasmic O-GlcNAc Modification of the Head Domain and the KSP Repeat Motif of the Neurofilament Protein Neurofilament-H. THE JOURNAL OF BIOLOGICAL CHEMISTRY *271*, 20845–20852.

Du, X.L., Edelstein, D., Dimmeler, S., Ju, Q., Sui, C., and Brownlee, M. (2001). Hyperglycemia inhibits endothelial nitric oxide synthase activity by posttranslational modification at the Akt site. The journal of Clinical Investigation *108*, 1341–1348.

Egan, D.F., Shackelford, D.B., Mihaylova, M.M., Gelino, S., Kohnz, R.A., Mair, W., Vasquez, D.S., Joshi, A., Gwinn, D.M., Taylor, R., *et al.* (2011). Phosphorylation of ULK1 (hATG1) by AMP-Activated Protein Kinase Connects Energy Sensing to Mitophagy. Science *331*, 456-461.

Gao, W., Shen, Z., Shang, L., and Wang, X. (2011). Upregulation of human autophagy-initiation kinase ULK1 by tumor suppressor p53 contributes to DNA-damage-induced cell death. Cell Death and Differentiation *18*, 1598–1607.

Griffith, L.S., Mathes, M., and Schmitz, B. (1995). p-Amyloid Precursor Protein Is Modified With 0-Linked N-Acetylglucosamine. Journal of Neuroscience Research *41*, 270-278.

Hanover, J.A., Krause, M.W., and Love, D.C. (2010). The hexosamine signaling pathway: O-GlcNAc cycling in feast or famine. Biochimica et Biophysica Acta *1800*, 80-95.

Hara, T., Takamura, A., Kishi, C., Iemura, S.I., Natsume, T., Guan, J.L., and Mizushima, N. (2008). FIP200, a ULK-interacting protein, is required for autophagosome formation in mammalian cells. The Journal of Cell Biology *181*, 497.

Hardie, D.G. (2007). AMP-activated/SNF1 protein kinases: conserved guardians of cellular energy. Nature *8*, 774-785.

Hart, G.W., Housley, M.P., and Slawson, C. (2007). Cycling of O-linked β-N-acetylglucosamine on nucleocytoplasmic proteins. Nature *446*, 1017-1022.

Hay, N., and Sonenberg, N. (2004). Upstream and downstream of mTOR. Genes & Dev *18*, 1926–1945.

Hosokawa, N., Hara, T., Kaizuka, T., Kishi, C., Takamura, A., Miura, Y., Iemura, S.I., Natsume, T., Takehana, K., Yamada, N., *et al.* (2011). Nutrient-dependent mTORC1 Association with the ULK1–Atg13–FIP200 Complex Required for Autophagy. Mol BIol Cell *20*, 1981-1991.

Hsu, P.P., Kang, S.A., Rameseder, J., Zhang, Y., Ottina, K.A., Lim, D., Peterson, T.R., Choi, Y., Gray, N.S., Yaffe, M.B., *et al.* (2011). The mTOR-Regulated Phosphoproteome Reveals a Mechanism of mTORC1-Mediated Inhibition of Growth Factor Signaling. Science *332*, 1317-1322.

Hwang, J.Y., Gertner, M., Pontarelli, F., Court-Vazquez, B., Bennett, M.V.L., Ofengeim, D., and Zukin, R.S. (2017). Global ischemia induces lysosomal-mediated degradation of mTOR and activation of autophagy in hippocampal neurons destined to die. Cell Death and Differentiation *24*, 317-329.

Itakura, E., Kishi-Itakura, C., and Mizushima, N. (2012). The Hairpin-type Tail-Anchored SNARE Syntaxin 17 Targets to Autophagosomes for Fusion with Endosomes/Lysosomes. Cell *151*, 1256–1269.

Itakura, E., Kishi, C., Inoue, K., and Mizushima, N. (2008). Beclin 1 forms two distinct phosphatidylinositol 3-kinase complexes with mammalian Atg14 and UVRAG. Molecular Biology of the Cell *19*, 5360-5372.

Itakura, E., and Mizushima, N. (2010). Characterization of autophagosome formation site by a hierarchical analysis of mammalian Atg proteins. Autophagy *6*, 764-776.

Jang, H.C., Kim T.W., Yoon, S.H., Choi, S.Y., Kang, T.W., Kim, S.Y., Kwon, Y.W., Cho, E.J., and Young, H.D. (2012). O-GlcNAcRegulates PluripotencyandReprogramming by Directly Acting on Core Components of the Pluripotency Network. Cell Stem Cell *11*, 62-74.

Julien, L.A., Carriere, A., Moreau, J., and Rou, P.P. (2010). mTORC1-Activated S6K1 Phosphorylates Rictor on Threonine 1135 and Regulates mTORC2 Signaling. Mol Cell Biol *30*, 908–921.

Jung, C.H., Jun, C.B., Ro, S.H., Kim, Y.M., Otto, N.M., Cao, J., Kundu, M., and and Kim, D.H. (2009). ULK-Atg13-FIP200 Complexes Mediate mTOR Signaling to the Autophagy Machinery. Mol BIol Cell *20*, 1992-2003.

Kamemura, K., Hayes, B.K., Comer, F.I., and Hart, G.W. (2002). Dynamic Interplay between O-Glycosylation and O-Phosphorylation of Nucleocytoplasmic Proteins. *277*, 19229–19235.

Kanwal, S., Fardini, Y., Pagesy, P., N'Tumba-Byn, T., Pierre-Eugène, C., Masson, E., , Hampe, C., and Issad, T. (2013). O-GlcNAcylation-Inducing Treatments Inhibit Estrogen Receptor α Expression and Confer Resistance Plos One *8*, 1-17.

Kim, D.H., King, J.E., Sarbassov, D.D., Latek, R.R., Erdjument-Bromage, H., and Sabatini, D.M. (2002). mTOR Interacts with Raptor to Form a Nutrient-Sensitive Complex that Signals to the Cell Growth Machinery. Cell *110*, 163–175.

Kim, J., Kim, Y.C., Fang, C., Russell, R.C., Kim, J.H., Fan, W., Liu, , R., Z., Q., , and Guan, K.L. (2013). Differential regulation of distinct VPS34 complexes by AMPK in nutrient stress and autophagy. Cell *152*, 290–303.

Kim, J., Kundu, M., Viollet, B., and Guan, K.L. (2011). AMPK and mTOR regulate autophagy through direct phosphorylation of Ulk1. Nature Cell Biology *13*, 132-141.

Lehman, D.M., Fu, D.J., Johnson-Pais, T., Goring, H.H.H., Freeman, A.B., Hamlington, J., Duggirala, R., Dyer, T.D., Arya, R., Blangero, J., *et al.* (2005). A Single Nucleotide Polymorphism in MGEA5 Encoding O-GlcNAc–selective N-Acetyl-ɴʟ-D Glucosaminidase Is Associated With Type 2 Diabetes in Mexican Americans. Diabetes *54*, 1214-1221.

Levine, B., and Deretic, V. (2007). Unveiling the roles of autophagy in innate and adaptive immunity. Nature Reviews Immunology *7*, 767.

Liang, C., Feng, P., Ku, B., Dotan, I., and Canaani, D. (2006). Autophagic and tumour suppressor activity of a novel Beclin1-binding protein UVRAG. Nature Cell Biology *8*, 688-699.

Mathew, R., Karantza-Wadsworth, V., and White, E. (2007). Role of autophagy in cancer. Nature Reviews Cancer *7*, 961-967.

Matsunaga, K., Saitoh, T., Tabata, K., Omori, H., and Satoh, T. (2009). Two Beclin 1-binding proteins, Atg14L and Rubicon, reciprocally regulate autophagy at different stages. Nature Cell Biology *11*, 385-396.

Medina, L., Grove, K., and Haltiwanger, R.S. (1998). SV40 large T antigen is modified with O-linked N-acetylglucosamine but not with other forms of glycosylation. Glycobiology *8*, 383–391.

Meley, D., Bauvy, C., Houben-Weerts, J.H.P.M., Codogno, P., and Meijer, A.J. (2006). AMP-activated Protein Kinase and the Regulation of Autophagic Proteolysis. THE JOURNAL OF BIOLOGICAL CHEMISTRY *281*, 34870–34879.

Menon, S., Dibble, C.C., Talbott, G., Hoxhaj, G., Valvezan, A.J., Takahashi, H., Cantley, L.C., and Manning, B.D. (2014). Spatial Control of the TSC Complex Integrates Insulin and Nutrient Regulation of mTORC1 at the Lysosome. Cell *156*, 771-785.

Misra, S., Miller, G.J., and Hurley, J.H. (2001). Recognizing Phosphatidylinositol 3-Phosphate. Cell *107*, 559-562.

Mizushima, N. (2005). The pleiotropic role of autophagy: from protein metabolism to bactericide. Cell Death and Differentiation *12*, 1535–1541.

Mizushima, N. (2007). Autophagy: process and function. Genes & Dev *21*, 2861–2873.

Mizushima, N., Levine, B., Cuervo, A.M., and Klionsky, D.J. (2008). Autophagy fights disease through cellular self-digestion. Nature *451*, 1069-1075.

Mizushima, N., Yoshimori, T., and Levine, B. (2010). Methods in Mammalian Autophagy Research. Cell *140*, 313-326.

Pankiv, S., Clausen, T.H., Lamark, T., Brech, A., Bruun, J.A., Outzen, H., Øvervatn, A., Bjørkøy, G., and Johansen, T. (2007). p62/SQSTM1 Binds Directly to Atg8/LC3 to Facilitate Degradation of Ubiquitinated Protein Aggregates by Autophagy. Journal of biological chemistry *2007*, 1-18.

Park, J.M., Jung, C.H., Seo, M., Otto, N.M., Grunwald, D., Kim, K.H., Moriarity, B., Kim, Y.M., Starker, C., and Nho, R.S., Voytas, D., and Kim, D.H. (2016). The ULK1 complex mediates MTORC1 signaling to the autophagy initiation machinery via binding and phosphorylating ATG14. Autophagy *12*, 547–564

Pattingre, S., Bauvy, C., Carpentier‖, S., Levade, T., Levine, B., and Codogno, P. (2008). Role of JNK1-dependent Bcl-2 phosphorylation in ceramideinduced macroautophagy. Journal of Biological Chemistry *284*, 2719-2728.

Proikas-Cezanne, T., Takacs, Z., Donnes, P., and Kohlbacher, O. (2015). WIPI proteins: essential PtdIns3P effectors at the nascent autophagosome. The Company of Biologists *128*,, 207–217.

Qu, X., Zou, Z., Sun, Q., Luby-Phelps, K., Cheng, P., Hogan, R.N., Gilpin, C., and Levine, B. (2007). Autophagy Gene-Dependent Clearance of Apoptotic Cells during Embryonic Development. Cell *128*, 931-946.

Ruan, H.B., Ma, Y., Torres, S., Zhang, B., Feriod, C., Heck, R.M., Qian, K., Fu, M., Li, X., Nathanson, M.H., *et al.* (2017). Calcium-dependent O-GlcNAc signaling drives liver autophagy in adaptation to starvation. Genes & Dev *31*, 1655-1665.

Russell, R.C., Tian, Y., Yuan, H., Park, H.W., Chang, Y.Y., Kim, J., Kim, H., Neufeld, T.Pl., Dillin, A., and Guan, K.L. (2013). ULK1 induces autophagy by phosphorylating Beclin-1 and activating VPS34 lipid kinase. Nature Cell Biology *15*, 741-750.

Schu, P.V., Takegawa, K., Fry, M.J., Stack, J.H., Waterfield, M.D., and Emr, S.D. (1993). Phosphatidylinositol 3-Kinase Encoded by Yeast VPS34 Gene Essential for Protein Sorting. Science *260*.

Shang, L., and Wang, X. (2011). AMPK and mTOR coordinate the regulation of Ulk1 and mammalian autophagy initiation. Autophagy *7*, 924-926.

Shang, L., and Wang, X. (2011). AMPK and mTOR coordinate the regulation of Ulk1 and mammalian autophagy initiation. Autophagy *7*, 924-926.

Slawson, C., and Hart, G.W. (2011). O-GlcNAc signalling: implications for cancer cell biology. Nature Reviews Cancer *11*, 678-684.

Slawson, C., Zachara, N.E., Vosseller, K., Cheung, W.D., Lane, M.D., and Hart, G.W. (2005). Perturbations in O-linked -N-Acetylglucosamine Protein Modification Cause Severe Defects in Mitotic Progression and Cytokinesis. THE JOURNAL OF BIOLOGICAL CHEMISTRY *280*, 32944–32956.

Sun, Q., Fan, W., Chen, K., Ding, X., Chen, S., and Zhong, Q. (2008). Identification of Barkor as a mammalian autophagy-specific factor for Beclin 1 and class III phosphatidylinositol 3-kinase. PNAS *105*, 19211–19216.

Takahashi, Y., Coppola, D., Matsushita, N., Cualing, H.D., Sun, M., Sato, Y., Liang, C., Jung, J.U., Cheng, J.Q., Mulé, J.J., *et al.* (2008). Bif-1 interacts with Beclin 1 through UVRAG and regulates autophagy and tumorigenesis. Nature Cell Biology *9*, 1142–1151.

Tarrant, M.K., Rho, H.S., Xie, Z., Jiang, Y.L., Gross, C., Culhane, J.C., Yan, G., Qian, J., Ichikawa, Y., Matsuoka, T., *et al.* (2012). Regulation of CK2 by phosphorylation and O-GlcNAcylation revealed by semisynthesis. Nature Chemical Biology *8*, 262-269.

Vocadlo, D.J. (2012). O-GlcNAc processing enzymes: catalytic mechanisms, substrate specificity, and enzyme regulation. Current Opinion in Chemical Biology *16*, 488-497.

Wang, Z., Gucek, M., and Hart, G.W. (2008). Cross-talk between GlcNAcylation and phosphorylation: Site-specific phosphorylation dynamics in response to globally elevated O-GlcNAc. PNAS *105*, 13793–13798.

Wells, L., Kreppel, L.K., Comer, F.I., Wadzinski, B.E., and Hart, G.W. (2004). O-GlcNAc transferase is in a functional complex with protein phosphatase 1 catalytic subunits. Journal of Biological Chemistry *279*, 38466-38470.

Wells, L., Vosseller, K., and Hart, G.W. (2001). Glycosylation of Nucleocytoplasmic Proteins: Signal Transduction and O-GlcNAc. Science *291*, 2376-2378.

Wong, P.M., Feng, Y., Wang, J., Shi, R., and Jiang, X. (2015). Regulation of autophagy by coordinated action of mTORC1 and protein phosphatase 2A. Nature Communications *6*.

Yan, J., Kuroyanagi, H., Kuroiwa, A., Matsuda, Y., Tokumitsu, H., Tomoda, T., Shirasawa, T., and and Muramatsu, M. (1998). Identification of Mouse ULK1, a Novel Protein Kinase Structurally Related to C. elegans UNC-51. BIOCHEMICAL AND BIOPHYSICAL RESEARCH COMMUNICATIONS, 222–227.

Yang, W.H., Kim, J.E., Nam, H.W., Ju, J.W., Kim, H.S., Kim, Y.S., and J.W., a.C. (2006). Modification of p53 with O-linked N-acetylglucosamine regulates p53 activity and stability. Nature Cell BIology *8*, 1074-1083.

Yang, X., Ongusaha, P.P., Miles, P.D., Havstad J.C., Zhang, F., So, W.V., Kudlow, J.E., Michell, R.H., Olefsky, J.M., Field, S.J., *et al.* (2008). Phosphoinositide signalling links O-GlcNAc transferase to insulin resistance. Nature *451*, 964-970.

Yi, W., Clark, P.M., Mason, D.E., Keenan, M.C., Hill, C., Goddard III, W.A., Peters, E.C., Driggers, E.M., and Hsieh-Wilson, L.C. (2012). Phosphofructokinase 1 Glycosylation Regulates Cell Growth and Metabolism. Science *337*, 975-980.

Yki-Jarvinen, H., Virkam, A., Daniels, M.C., McClain, D., and Gottschalk, W.K. (1998). Insulin and Glucosamine Infusions Increase O-Linked N-Acetyl-Glucosamine in Skeletal Muscle Proteins In Vivo Metabolism *47*, 449-455.

Zachara, N.E., and Hart, G.W. (2004). O-GlcNAc a sensor of cellular state: the role of nucleocytoplasmic glycosylation in modulating cellular function in response to nutrition and stress. Biochimica et Biophysica Acta *1673*, 13-28.

Zalckvar, E., Berissi, H., Mizrachy, L., Idelchuk, Y., Koren, I., Eisenstein, M., Sabanay, H., Pinkas-Kramarski, R., and Kimchi, A. (2009). DAP-kinase-mediated phosphorylation on the BH3 domain of beclin 1 promotes dissociation of beclin 1 from Bcl-XL and induction of autophagy. EMBO reports *10*, 285-292.

Zeidan, Q., and Hart, G.W. (2010). The intersections between O-GlcNAcylation and phosphorylation: implications for multiple signaling pathways. J Cell Sci *2010*, 13-22.

Zhong, Y., Wang, Q.J., Li, X., Yan, Y., Backer, J.M., Chait, B.T., Heintz, N., and Yue, Z. (2009). Distinct regulation of autophagic activity by Atg14L and Rubicon associated with Beclin 1-phosphatidylinositol-3-kinase complex. Nature Cell Biology *11*, 468-476.

Zhu, G., Tao, T., Zhang, D., Liu, X., Qiu, H., Han, L., Xu, Z., Xiao, Y., Cheng, C., and Shen, A. (2016). O-GlcNAcylation of histone deacetylase-1 in hepatocellular carcinoma promotes cancer progression. Glycobiology *26*, 820-833.

Zoncu, R., Efeyan, A., and Sabatini, D.M. (2011). mTOR: from growth signal integration to cancer, diabetes and ageing. Nature Reviews *12*, 21-35.

국문초록

(Abstract in Korean)

서울대학교 대학원

생명과학부

표기은

ULK1은 세린잔기와 트레오닌 잔기를 인산화 시키는 인산화효소로서 두 개의 인산화효소인 mTOR와 AMPK에 의한 조절을 받는다. 평소에는 mTOR에 의해 인산화 되고 있다가 영양분이 결핍 되었을 때 AMPK가 mTOR를 억제하고 ULK1을 인산화 시키면서 ULK1은 활성화 되며 BECLIN1, ATG13등의 타겟을 인산화 시키면서 자가포식작용의 개시를 촉진한다. 본 논문에서는 당 결핍 상황에서 ULK1이 OGT에 의해 T754 사이트에 당화가 된다는 것을 밝혔다. 흥미롭게도 ULK1의 당화는 근처에 존재하는 mTOR 의존적인 인산화가 탈인산화가 된 이후에 일어났다. 이는 OGT와 함께 콤플렉스를 이룬다고 알려진 PP1에 의한 탈인산화인 것으로 밝혔다. 그와 더불어 당 결핍 상황에서 AMPK에 의한 인산화가 ULK1 당화에 중요한 전제조건임을 밝혔다. ULK1의 당화는 ATG14L의 인산화에 중요하며 이는 지질 인산화 효소인 VPS34의 활성화로

이어지는 것을 확인 하였다. 이를 통해 PI(3)P가 생성되어 자가포식작용의 초기 단계인 파고포어 형성을 촉진하며 WIPI1이 파고포어로 올 수 있게 해준다는 것을 규명하였다. 이를 통해 ULK1의 당화는 자가포식작용의 초기 진행을 돕는다는 것을 밝혔다. 본 연구는 당 결핍 상황에서 에너지센서로 알려진 mTOR, AMPK, OGT에 의해 미세하게 변형 및 조절되는 ULK1의 기작을 밝혔으며, mTOR이 비활성화 될 때 탈인산화 효소와 같이 작용함으로서 수동적인 탈인산화가 아닌 탈인산화 효소에 의한 적극적인 조절 기작이 존재한다는 사실을 밝혔다. 또한 최초로 탈인산화효소와 OGT의 크로스톡의 실질적인 예시를 규명하였으며 차후 자가포식작용 및 당화에 의존적인 질병 치료와 관련, 신약 개발에 중요한 개념을 제시하였다.

주요어

자가포식작용, ULK1, OGT, mTOR, AMPK, PP1

학번: 2010-23128